Nanoparticles:
Syntheses, Quantum Confinement, Forces, and Nanobio Aspects

Summarized by
Prof. Dong June Ahn
Korea University

(Cited materials from Atkins and available in an internet space)

Contents

- Particles: Energy & Force
- Quantum Confinement Properties
- Nanoparticle Syntheses
- Size Control
- Shape Control
- Nanobio Aspects

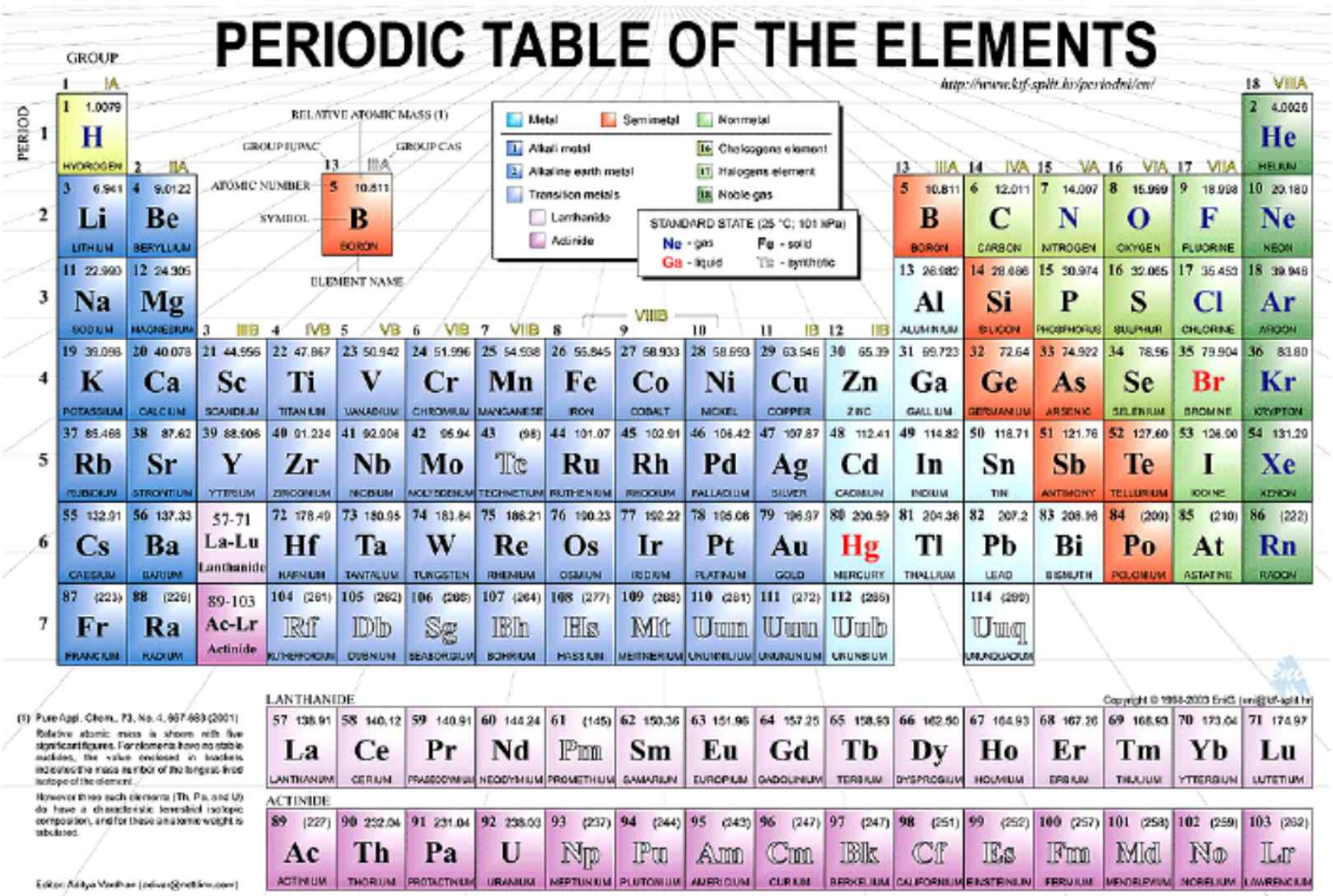

Atom vs. Molecule vs. "Nano"

Table F.3 Common SI prefixes

Prefix	y	z	a	f	p	n	μ	m	c	d
Name	yocto	zepto	atto	femto	pico	nano	micro	milli	centi	deci
Factor	10^{-24}	10^{-21}	10^{-18}	10^{-15}	10^{-12}	10^{-9}	10^{-6}	10^{-3}	10^{-2}	10^{-1}
Prefix	**da**	**h**	**k**	**M**	**G**	**T**	**P**	**E**	**Z**	**Y**
Name	deca	hecto	kilo	mega	giga	tera	peta	exa	zeta	yotta
Factor	10	10^{2}	10^{3}	10^{6}	10^{9}	10^{12}	10^{15}	10^{18}	10^{21}	10^{24}

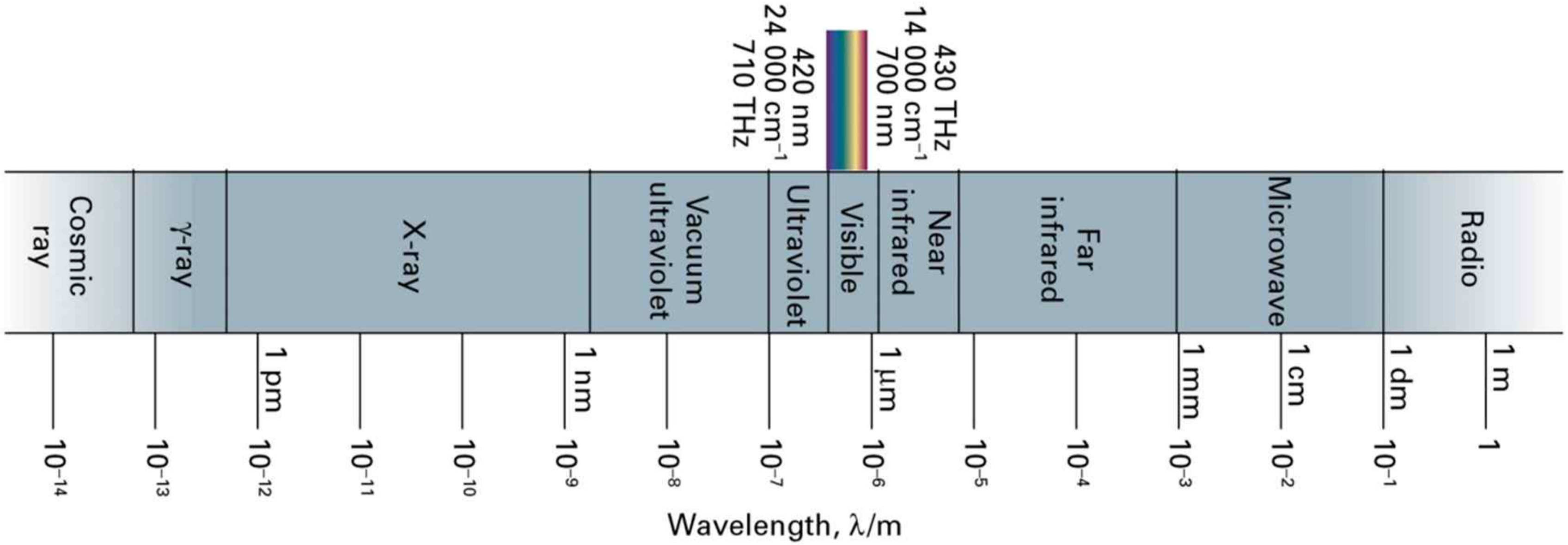

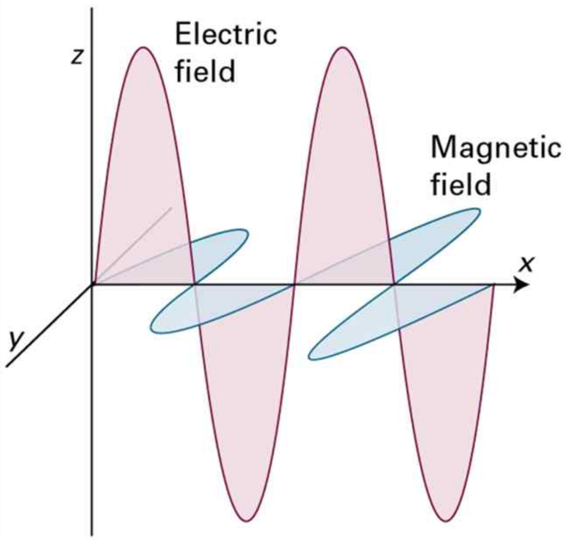

Spectral region	VHF	UHF	Microwave	Infrared	Visible	Ultraviolet	X-rays	γ-rays
Common usage	NMR	EPR	rotational transitions	vibrational transitions	electronic transitions		ionisation	nuclear effects
Frequency (Hz)	5×10^{8}	3×10^{10}	3×10^{11}	3×10^{13}	6×10^{14}	1.2×10^{15}	3.0×10^{17}	1.5×10^{19}
Wavelength	0.6 m	1 cm	1 mm	10 μm	500 nm	250 nm	1 nm	20 pm
Wavenumber (cm^{-1})	0.017	1.0	10.0	1000	20,000	40,000	1.0×10^{7}	5.0×10^{8}
Single photon energy (eV)	2.07×10^{-6}	1.24×10^{-4}	1.24×10^{-3}	1.24×10^{-1}	2.5	5.0	1.24×10^{3}	6.2×10^{4}
Photon energy ($kJ\ mol^{-1}$)	2.03×10^{-4}	1.20×10^{-2}	1.20×10^{-1}	12.0	239	479	1.2×10^{5}	6×10^{6}

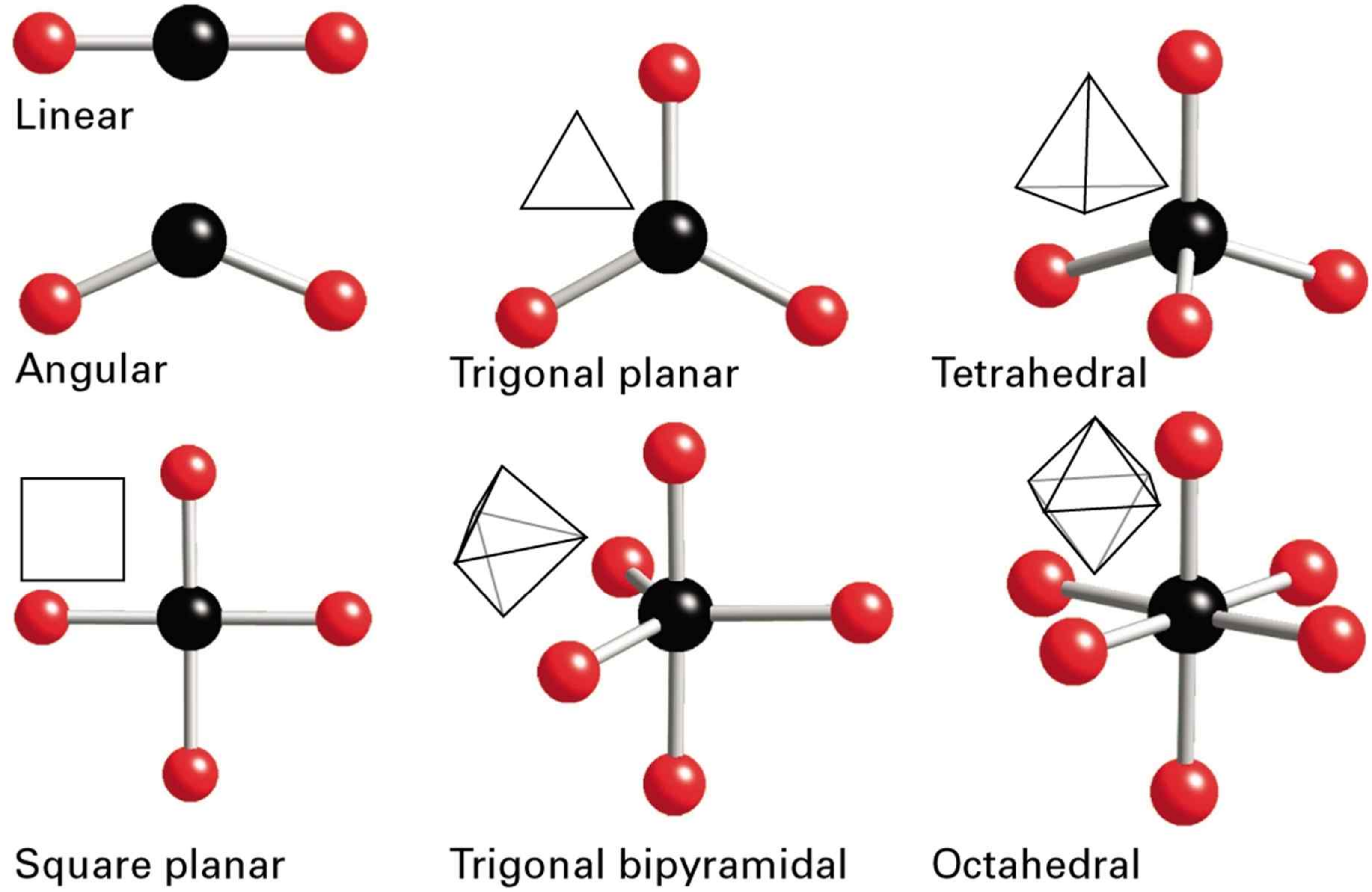
Linear
Angular
Trigonal planar
Tetrahedral
Square planar
Trigonal bipyramidal
Octahedral

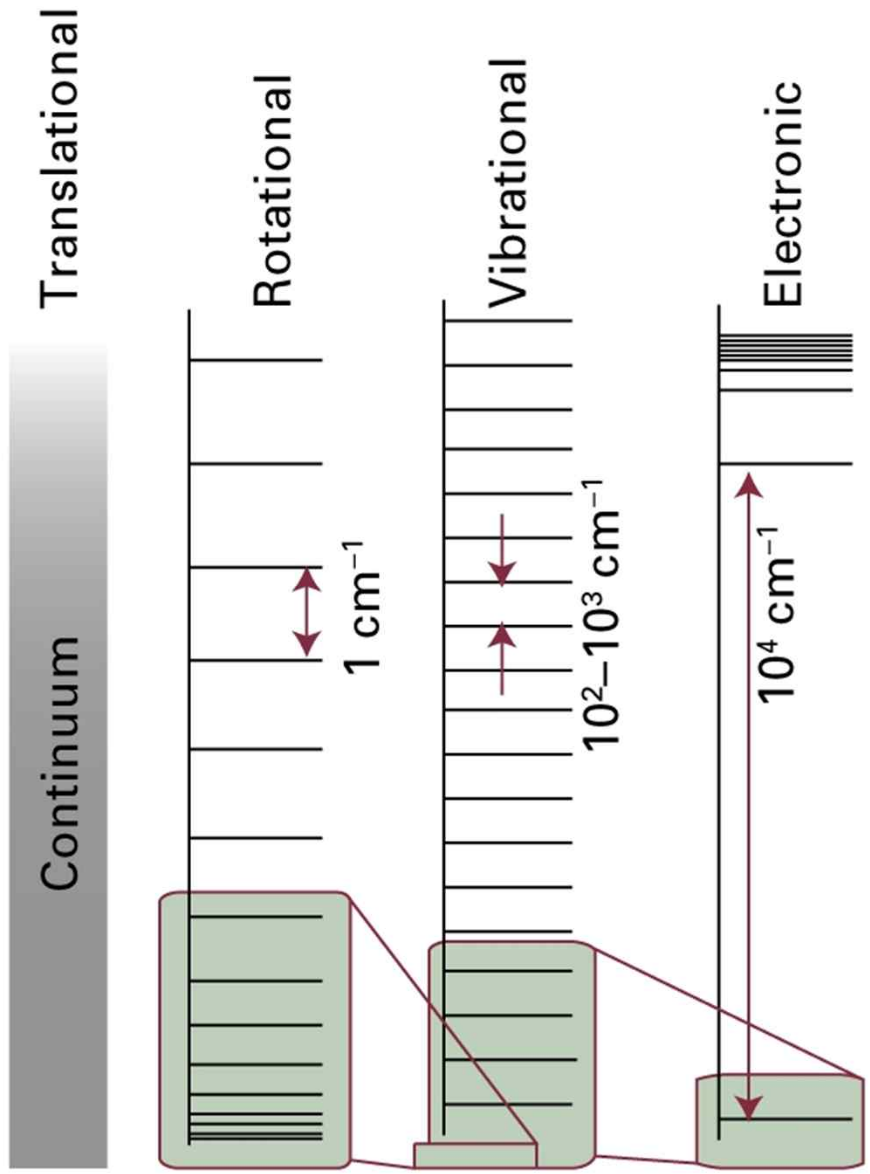
Translational
Continuum
Rotational
1 cm⁻¹
Vibrational
10²–10³ cm⁻¹
Electronic
10⁴ cm⁻¹

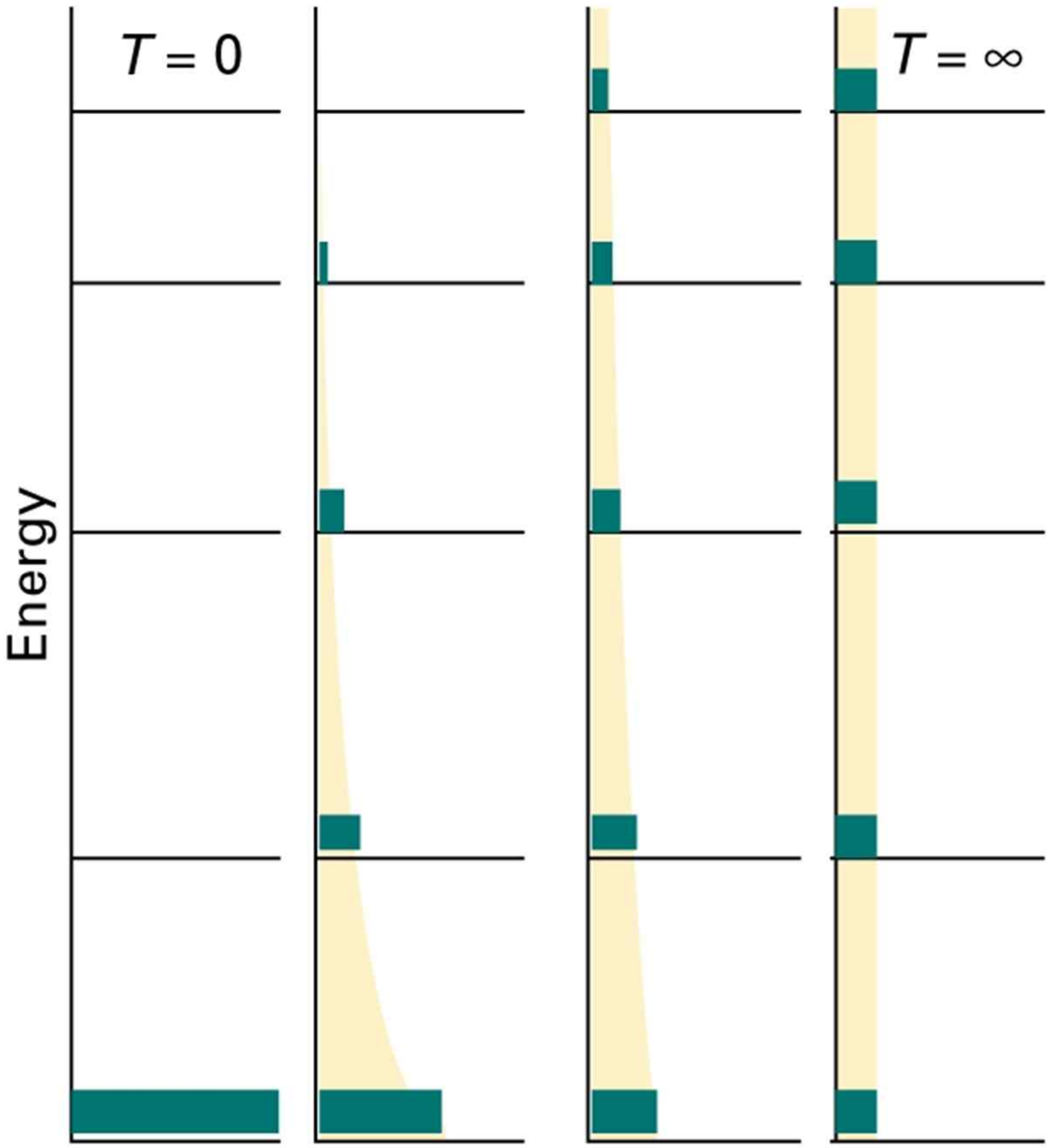
T = 0
T = ∞
Energy

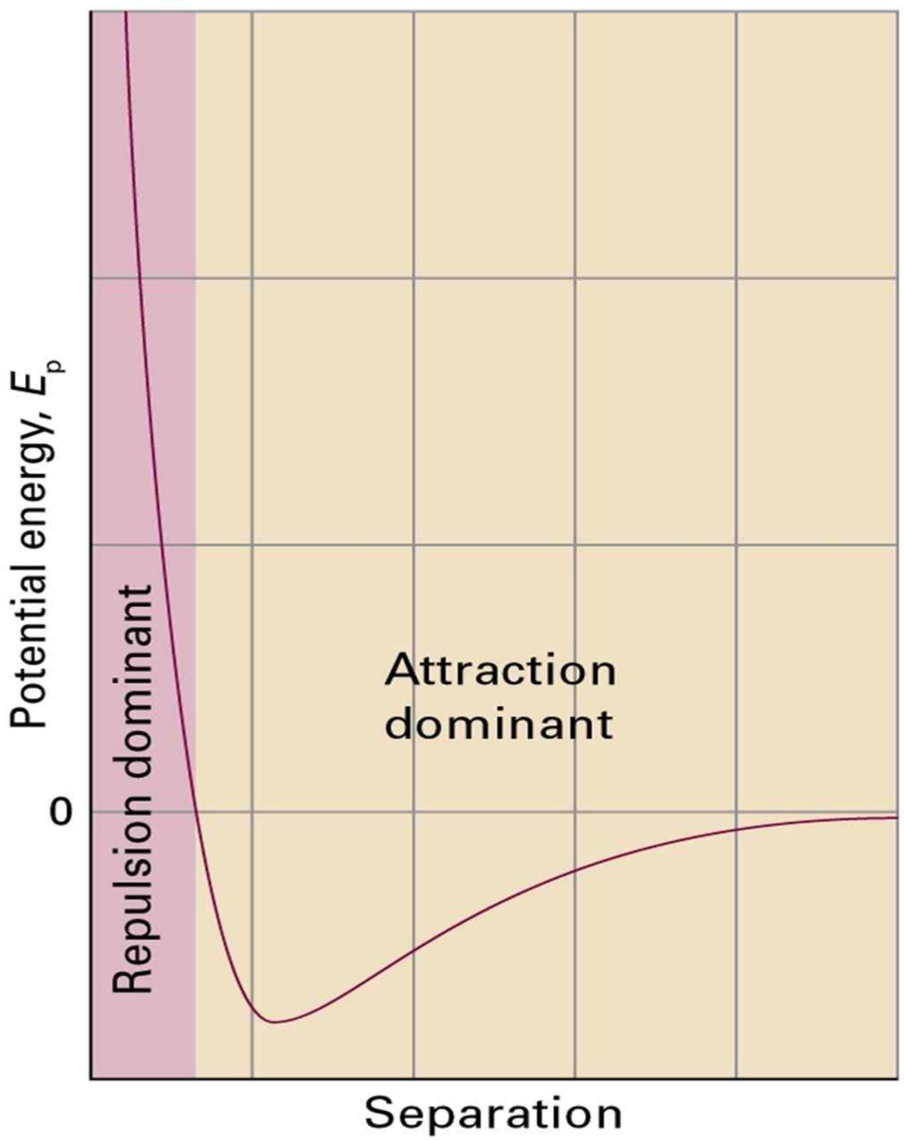

Potential energy, E_p
0
Repulsion dominant
Attraction dominant
Separation

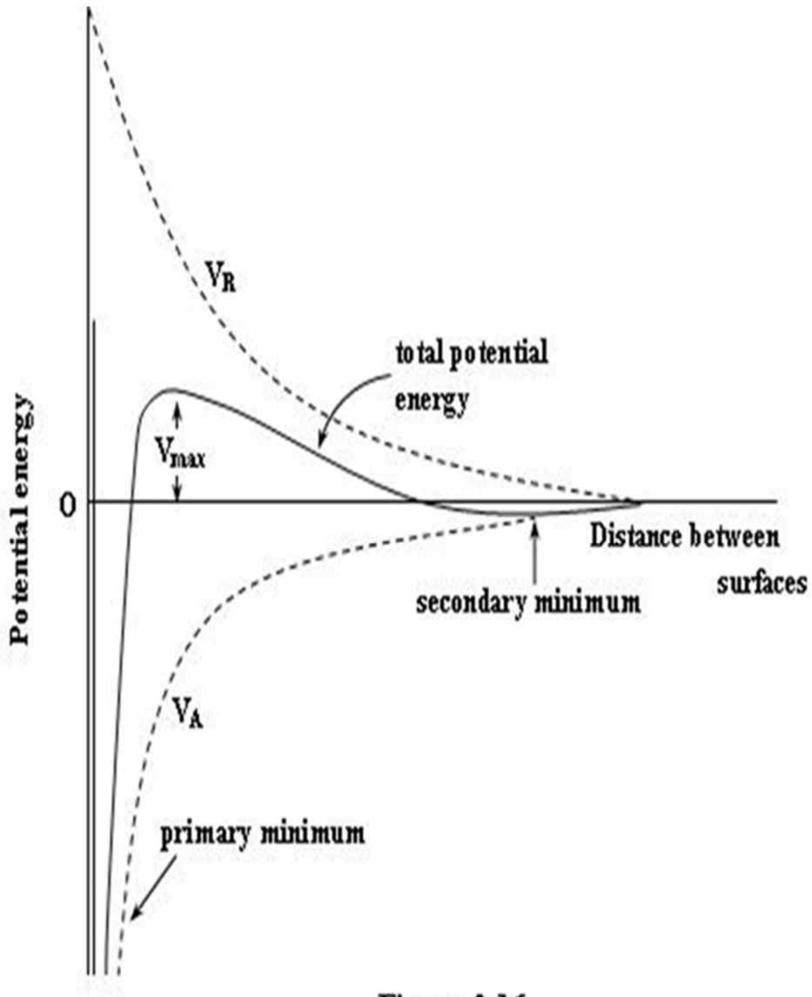
V_R
total potential
energy
V_max
0
Potential energy
Distance between
surfaces
secondary minimum
V_A
primary minimum

Figure 2.16

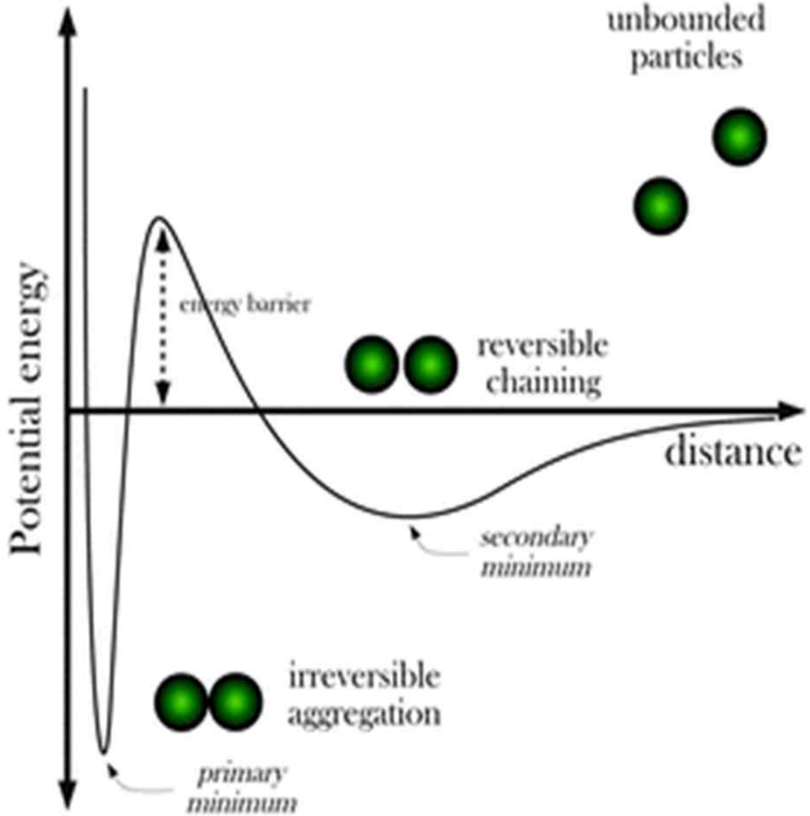
unbounded
particles
Potential energy
energy barrier
reversible
chaining
distance
secondary
minimum
irreversible
aggregation
primary
minimum

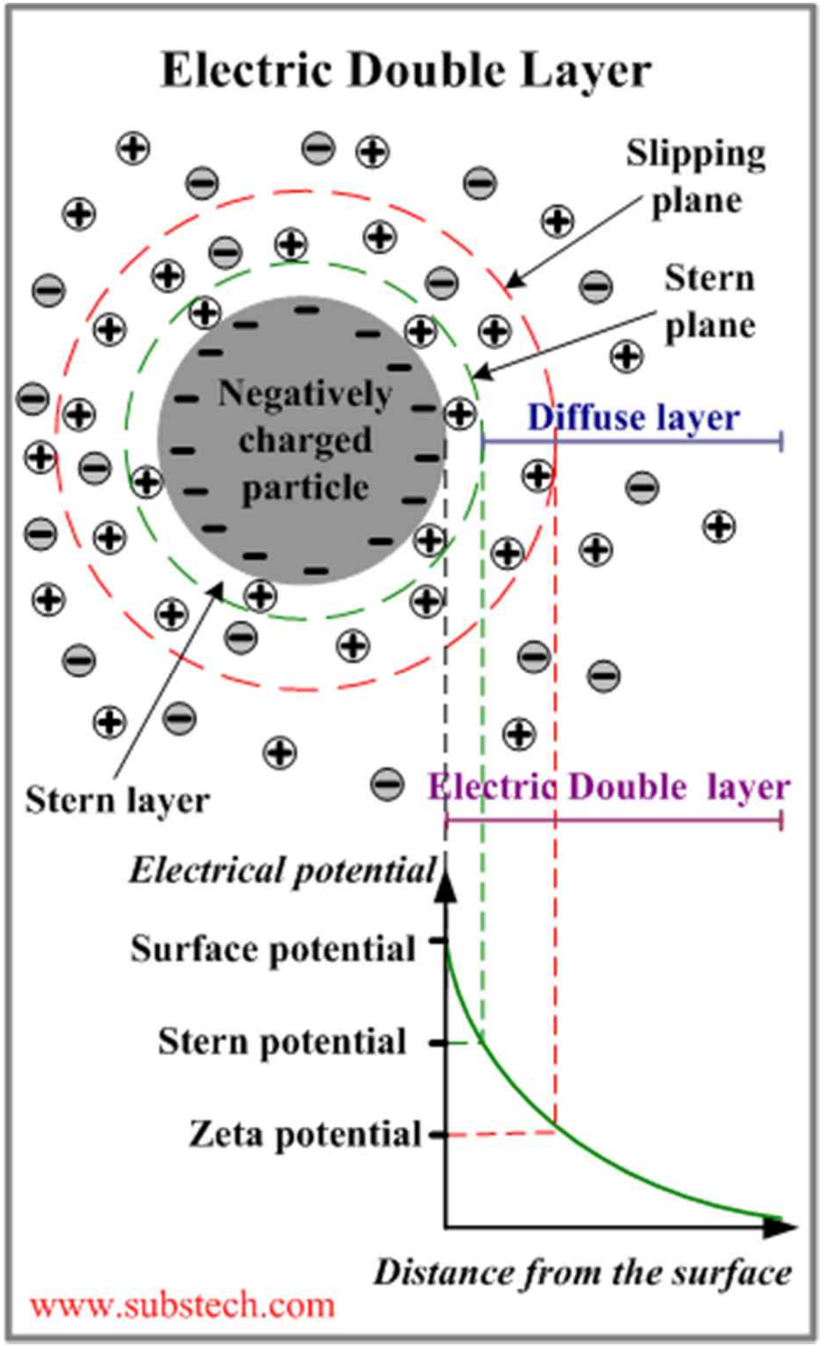
Electric Double Layer
Slipping plane
Stern plane
Negatively charged particle
Diffuse layer
Stern layer
Electric Double layer
Electrical potential
Surface potential
Stern potential
Zeta potential
Distance from the surface
www.substech.com

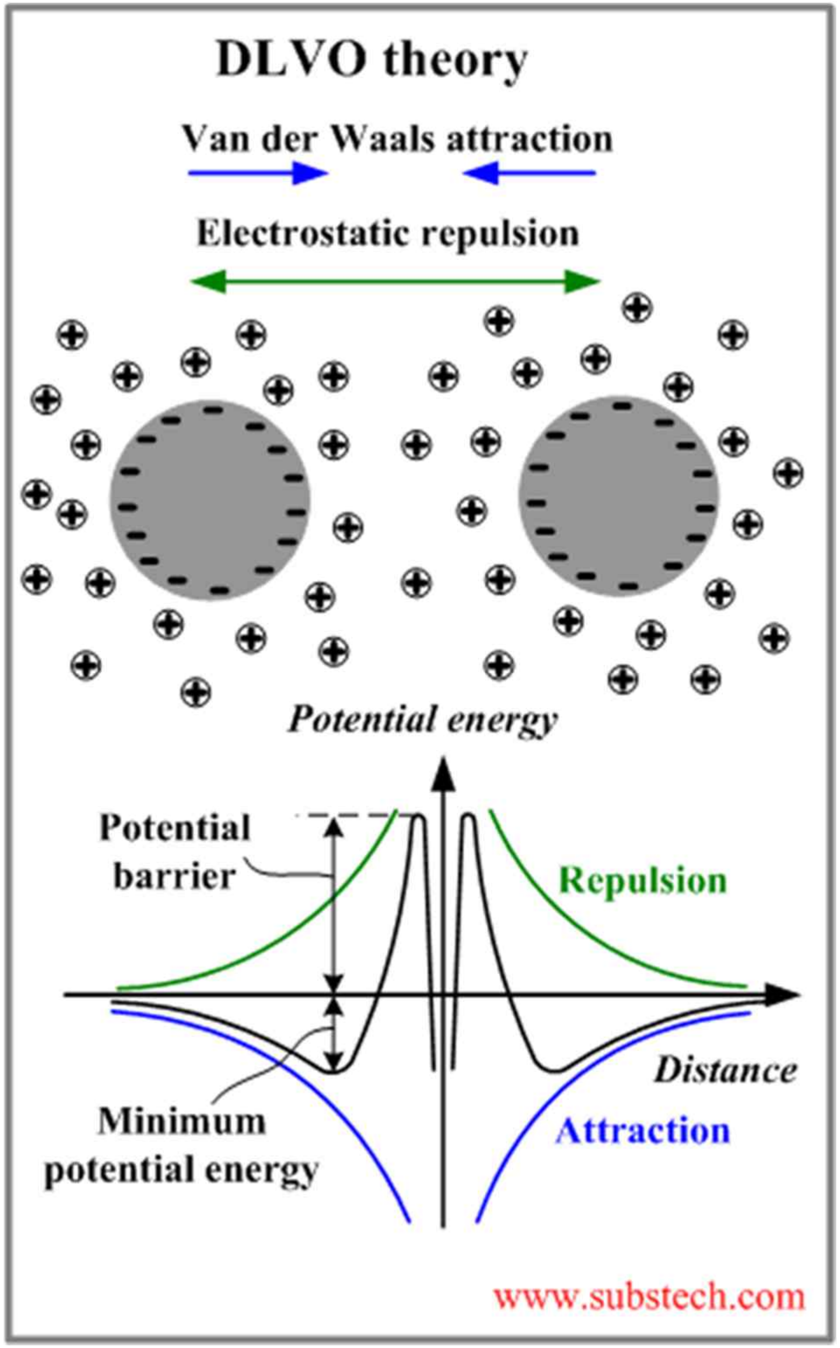
DLVO theory
Van der Waals attraction
Electrostatic repulsion
Potential energy
Potential barrier
Repulsion
Distance
Minimum potential energy
Attraction
www.substech.com

Nanocrystal

C-sixty
1nm

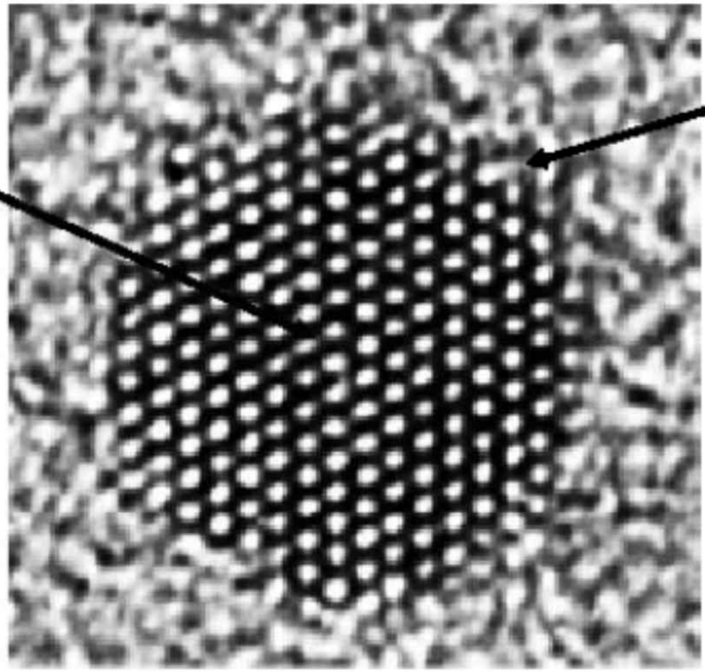

Cadmium Selenide nanocrystal
6 nm

Lysozyme
3 nm

Nanoparticle Synthesis

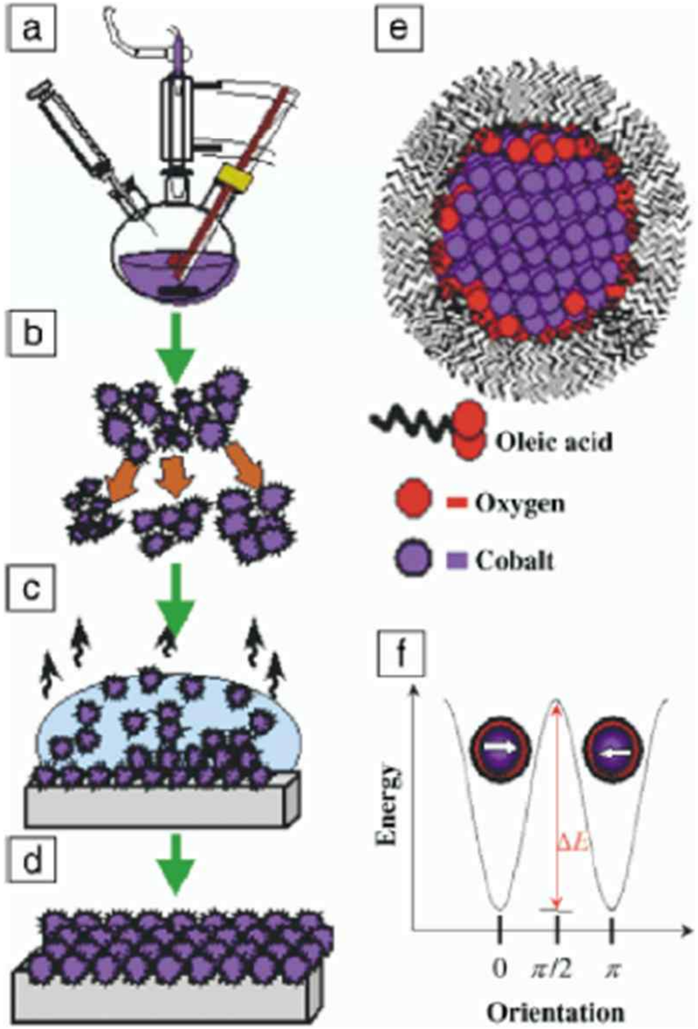

(a) nanoparticle (NP) synthesis by high-temperature solution-phase routes

(b) size-selective precipitation, used to narrow NP sample-size distributions;

(c) self-assembly of NP dispersions; and (d) formation of ordered NP assemblies (superlattices).

(e) Model nanoparticle with its close-packed metallic core, oxidized surface, and a monolayer coat of organic stabilizers (surfactants).

https://www.youtube.com/watch?v=bNuoYm7Su4o

Quantum Confinement Effect

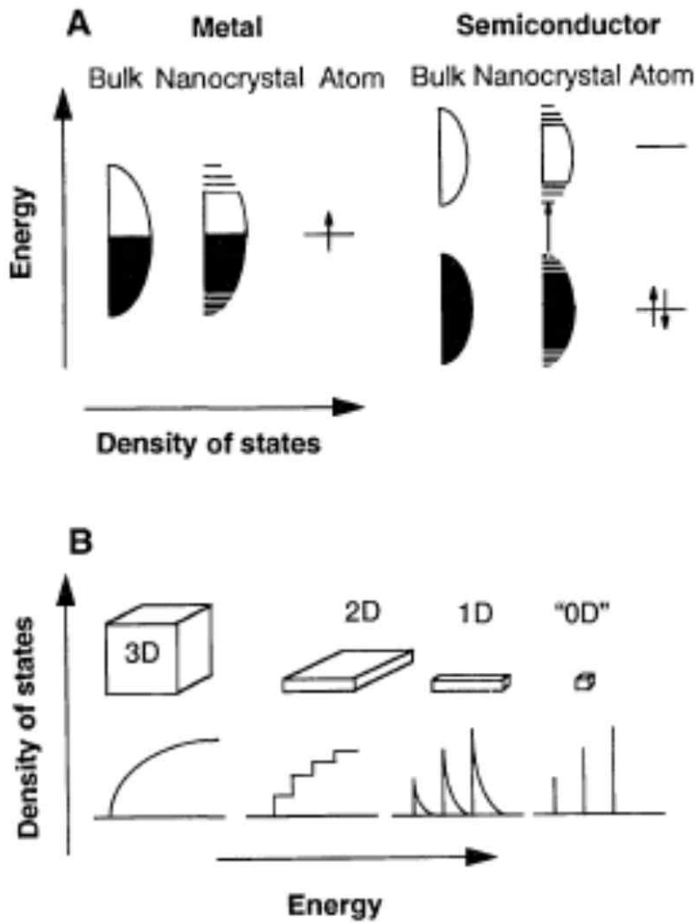

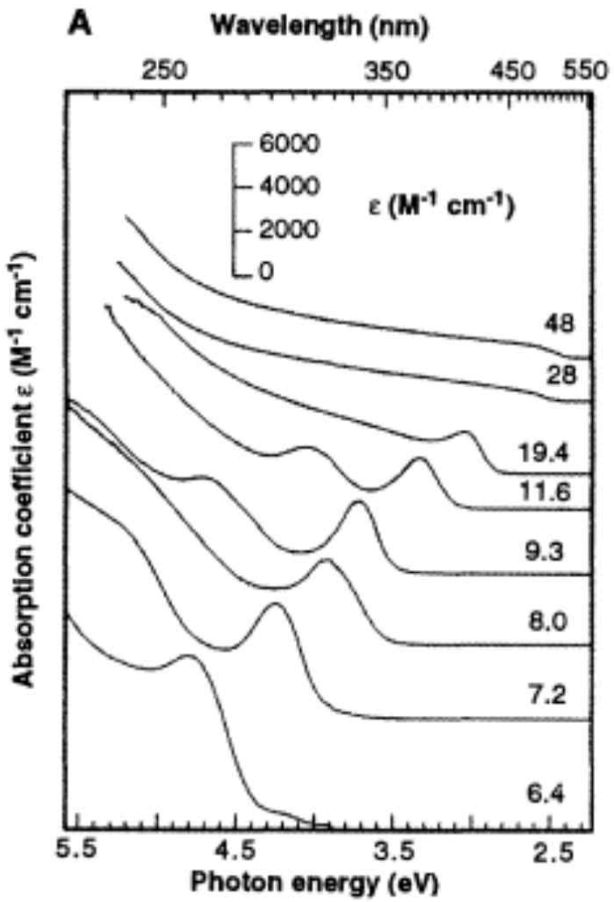

A. P. Alivisatos, Science, 271, 933-937 (1996)

Quantum dots of increasing size emit at different colors

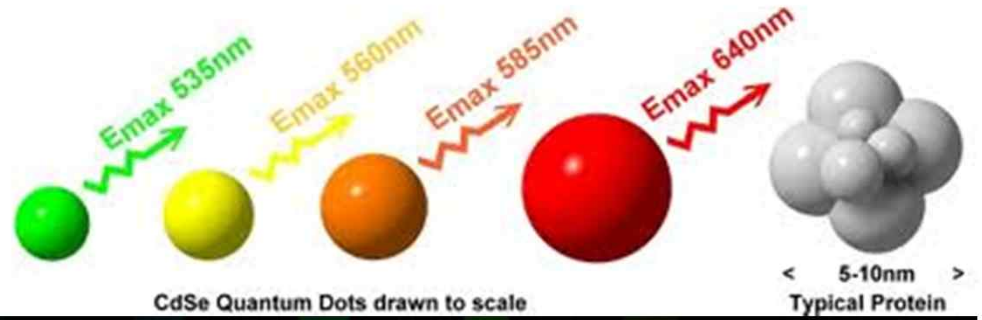

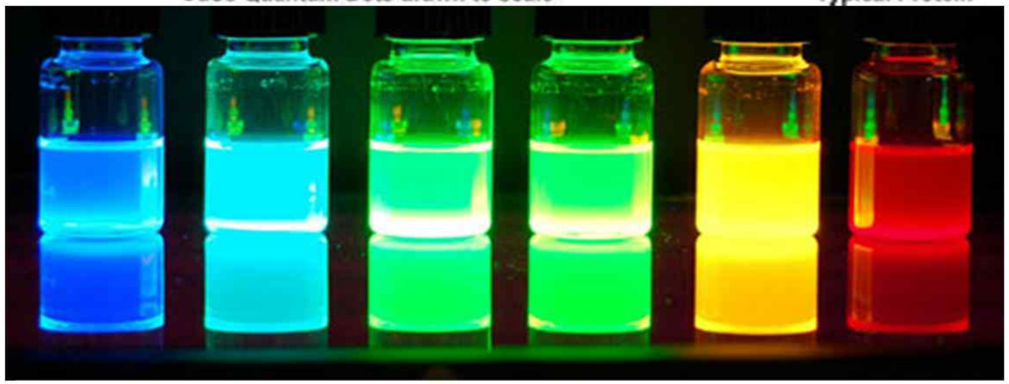

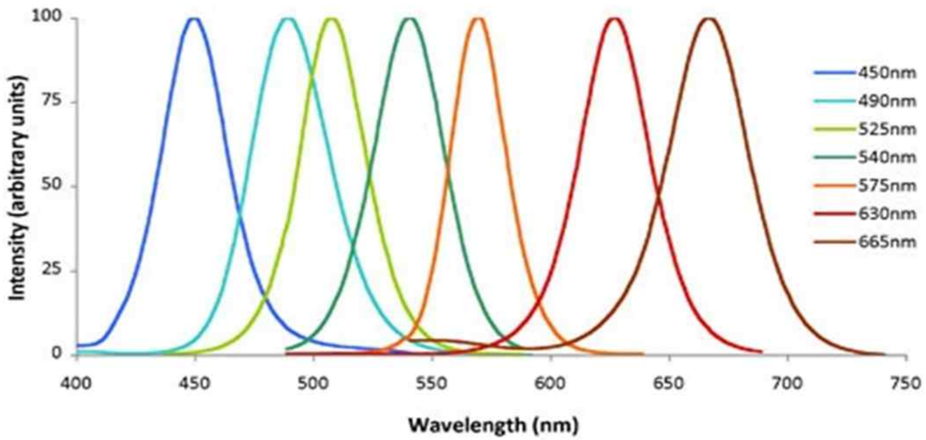

Band Theory on Quantum Confinement Effect

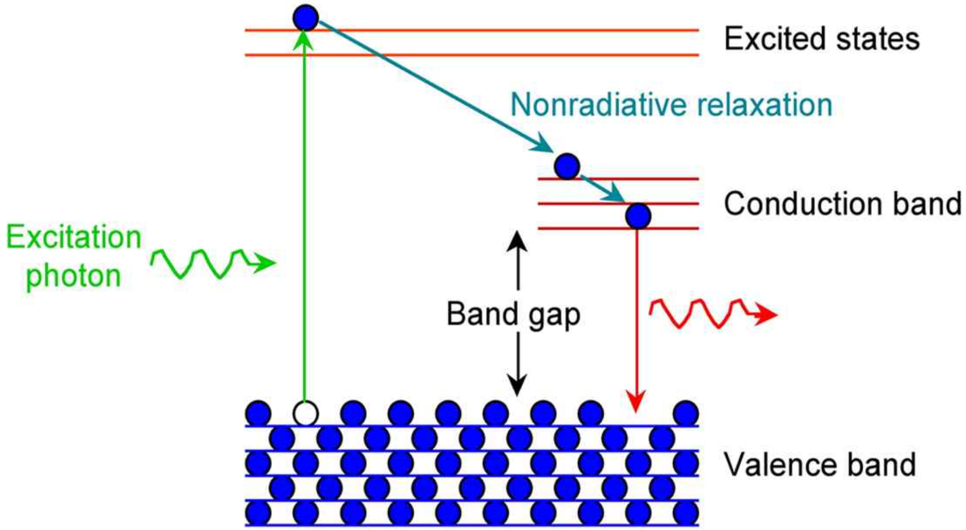

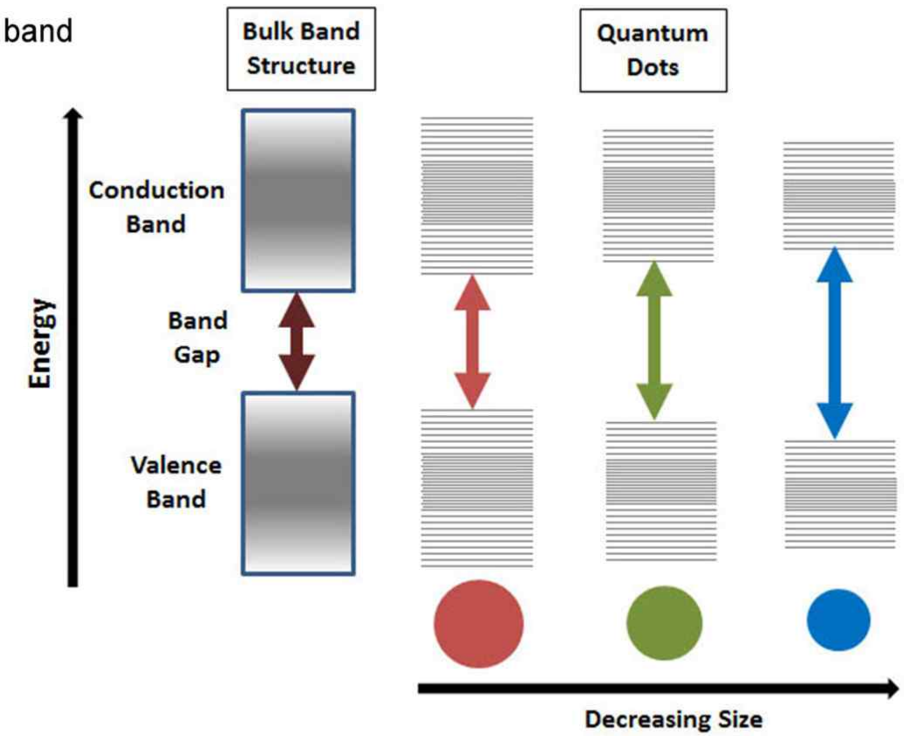

Molecular Photophysical Processes Relevant for Photobiology: Jablonski Diagram

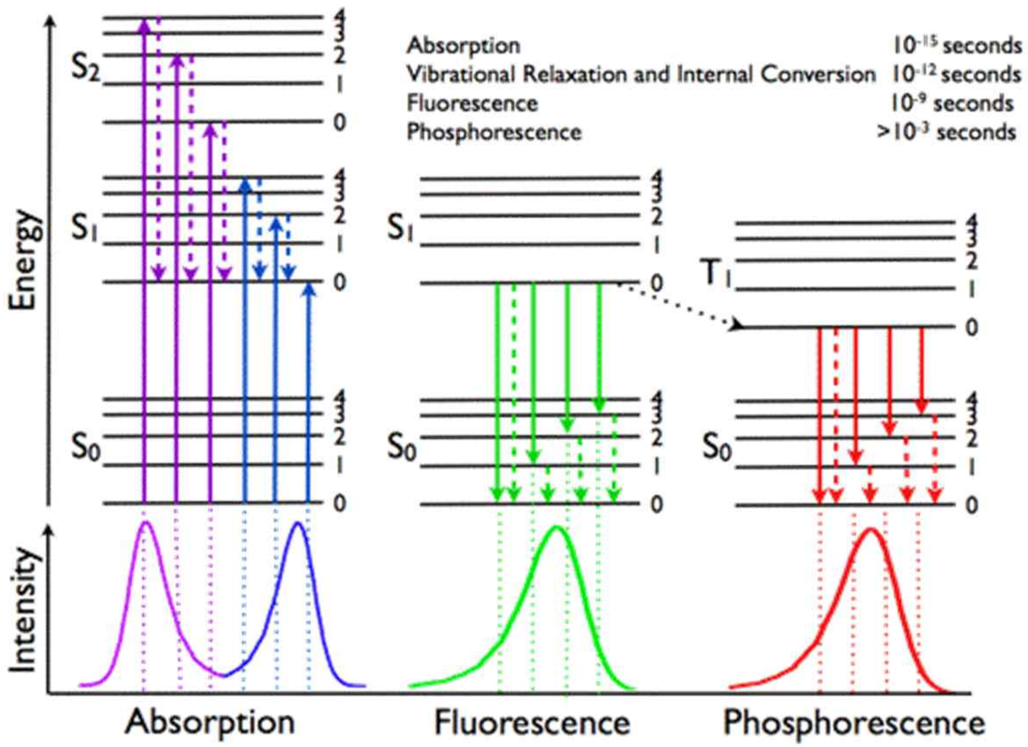

Jablonski diagram representing energy levels and spectra. Solid arrows indicate radiative transitions as occurring by absorption (violet, blue) or emission (green for fluorescence; red for phosphorescence) of a photon. Dashed arrows represent non-radiative transitions (violet, blue, green, red). Internal conversion is a non-radiative transition, which occurs when a vibrational state of a higher electronic state is coupled to a vibrational state of a lower electronic state. In the notation of, for example, S**1,0**, the first subscript refers to the electronic state (first excited) and the second one to the vibrational sublevel (v = 0). In the diagram the following internal conversions are indicated: S**2,4**→S**1,0**, S**2,2**→S**1,0**, S**2,0**→S**1,0** and S**1,0**→S**0,0**. The dotted arrow from S**1,0**→T**1,0** is a non-radiative transition called intersystem crossing, because it is a transition between states of different spin multiplicity. Below the diagram sketches of absorption-, fluorescence- and phosphorescence spectra are shown.

Photoluminescence

Photoluminescence is the emission of light from any material due to the loss of energy from excited state to ground state. There are two main types of luminescence – fluorescence and phosphorescence.

Fluorescence is a fast decay process, where the emission rate is around 10^8 s^{-1} and the lifetime is around 10^{-9} - 10^{-7} s. Fluorescence occurs when the excited state electron has an opposite spin compared to the ground state electrons. From the laws of quantum mechanics, this is an allowed transition, and occurs rapidly by emission of a photon. Fluorescence disappears as soon as the exciting light source is removed. Group 12-16 semiconductor quantum dots exhibit fluorescence properties when excited with ultraviolet light.

Phosphorescence is the emission of light, in which the excited state electron has the same spin orientation as the ground state electron. This transition is a forbidden one and hence the emission rates are slow (10^3 - 10^0 s^{-1}). So the phosphorescence lifetimes are longer, typically seconds to several minutes, while the excited phosphors slowly returned to the ground state. Phosphorescence is still seen, even after the exciting light source is removed.

Barron, A. Physical Methods in Chemistry and Nano Science, OpenStax_CNX Web site.
http://cnx.org/content/col10699/1.18/, Jan 3, 2014.

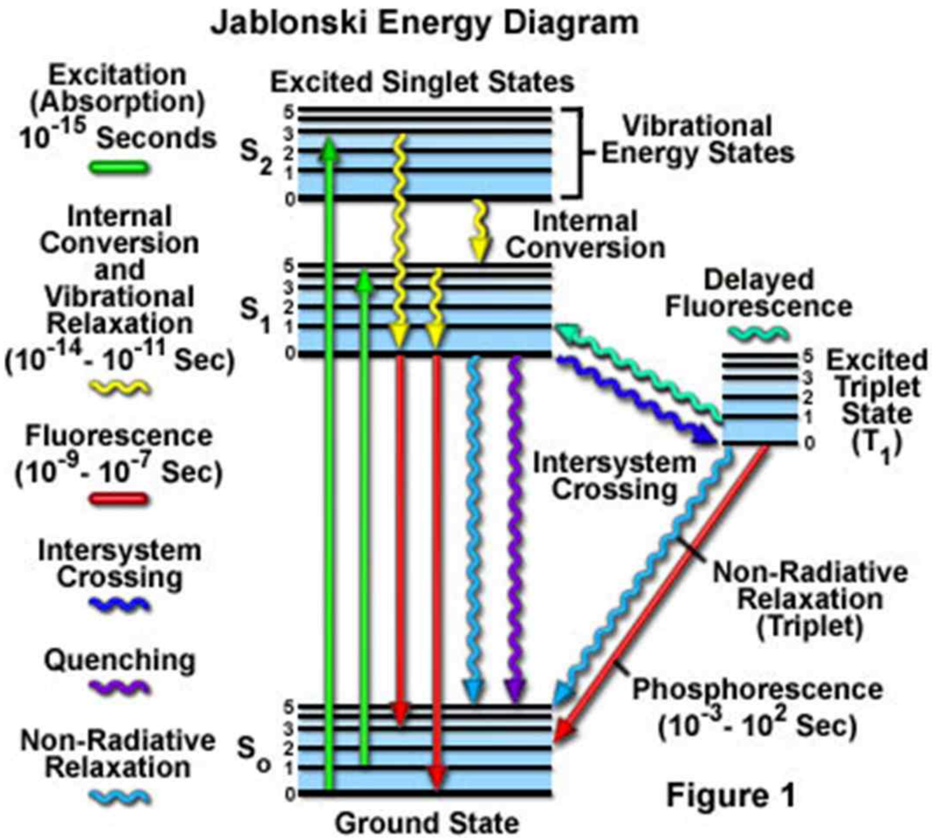

Jablonski Energy Diagram
Excitation (Absorption) 10^{-15} Seconds
Internal Conversion and Vibrational Relaxation (10^{-14} - 10^{-11} Sec)
Fluorescence (10^{-9} - 10^{-7} Sec)
Intersystem Crossing
Quenching
Non-Radiative Relaxation
Excited Singlet States
S_2
S_1
S_o
Vibrational Energy States
Internal Conversion
Delayed Fluorescence
Excited Triplet State (T_1)
Intersystem Crossing
Non-Radiative Relaxation (Triplet)
Phosphorescence (10^{-3} - 10^{2} Sec)
Ground State

Figure 1

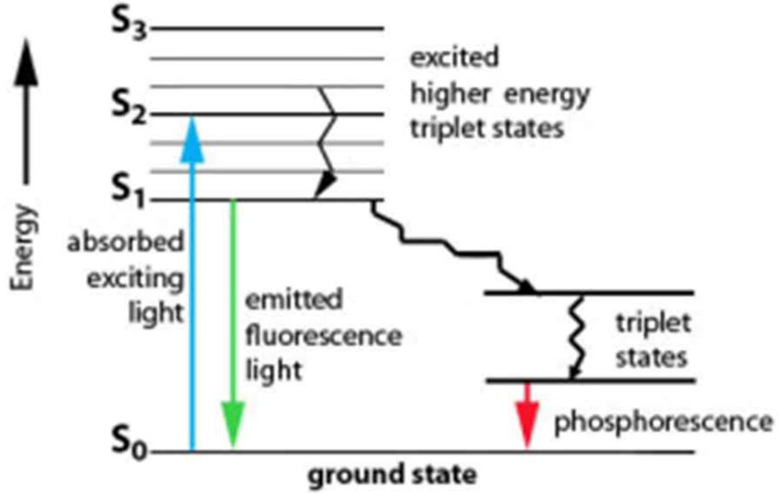

Energy
S_3
S_2
S_1
S_0
excited higher energy triplet states
absorbed exciting light
emitted fluorescence light
triplet states
phosphorescence
ground state

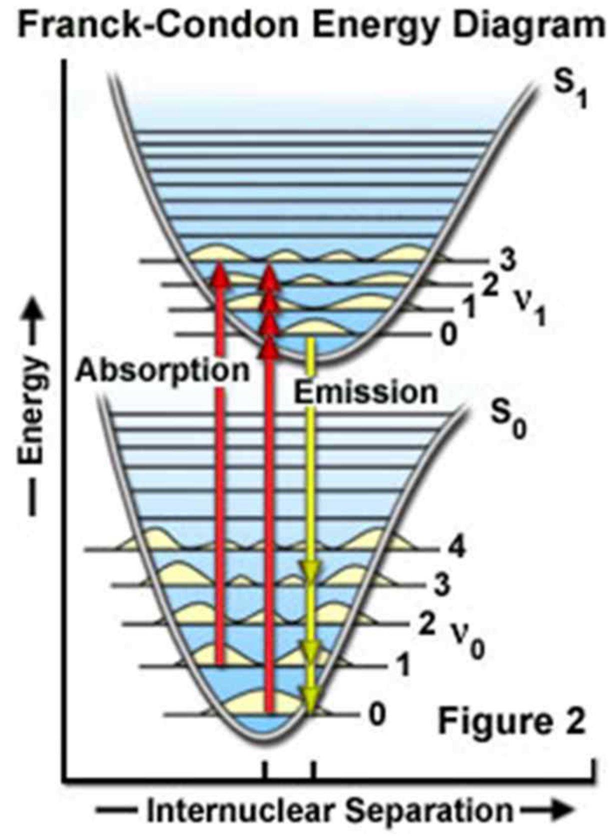

Figure 2

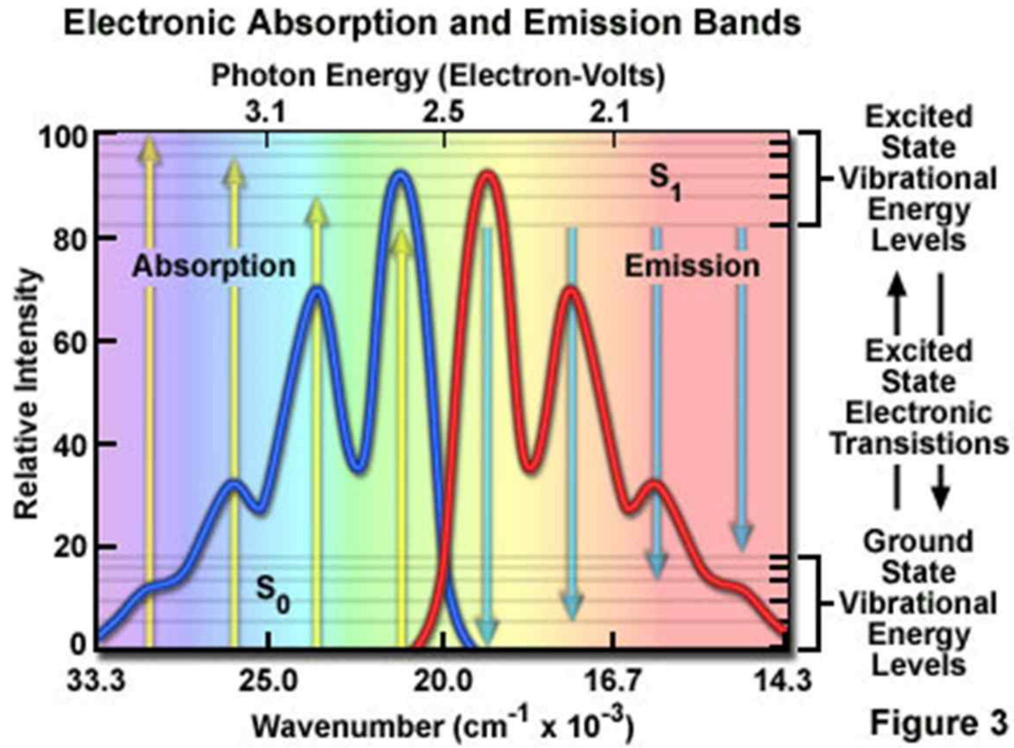

Figure 3

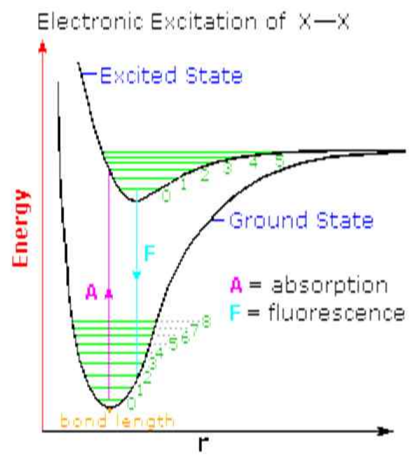

Resonance Energy Transfer from Donor to Acceptor

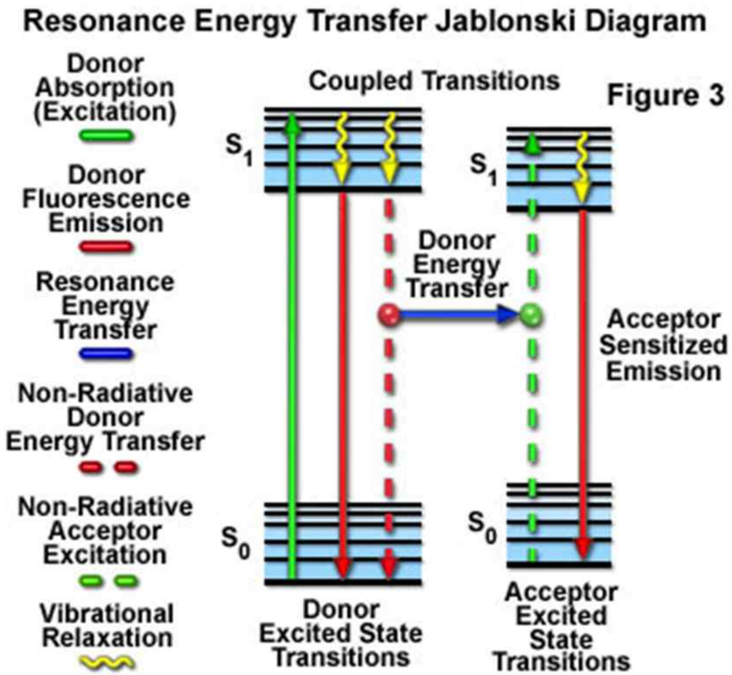

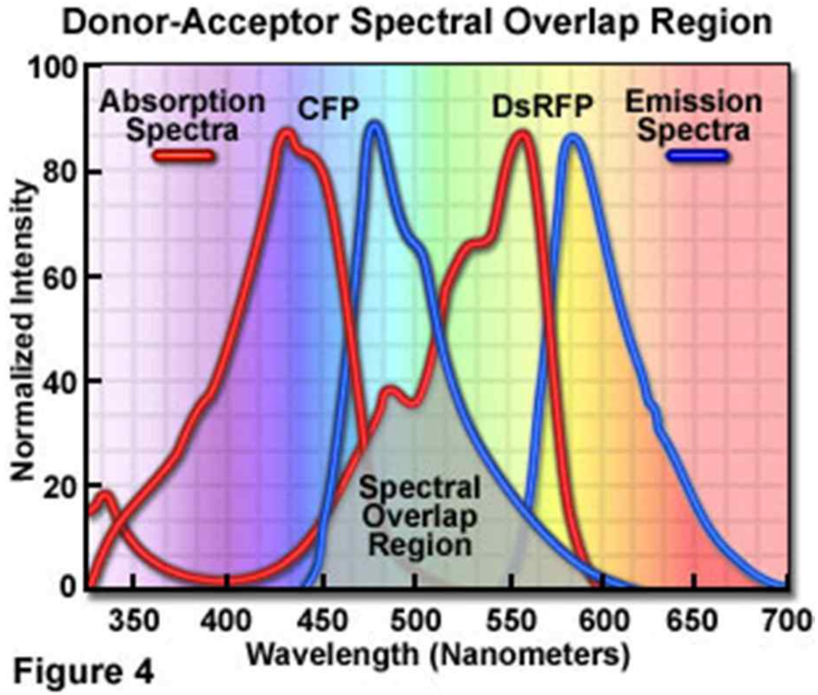

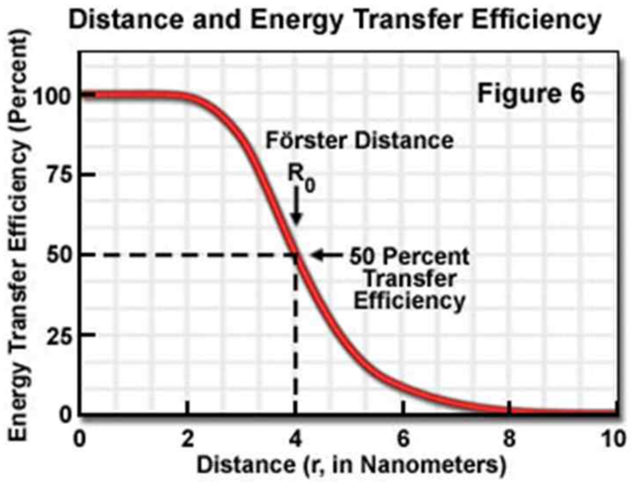

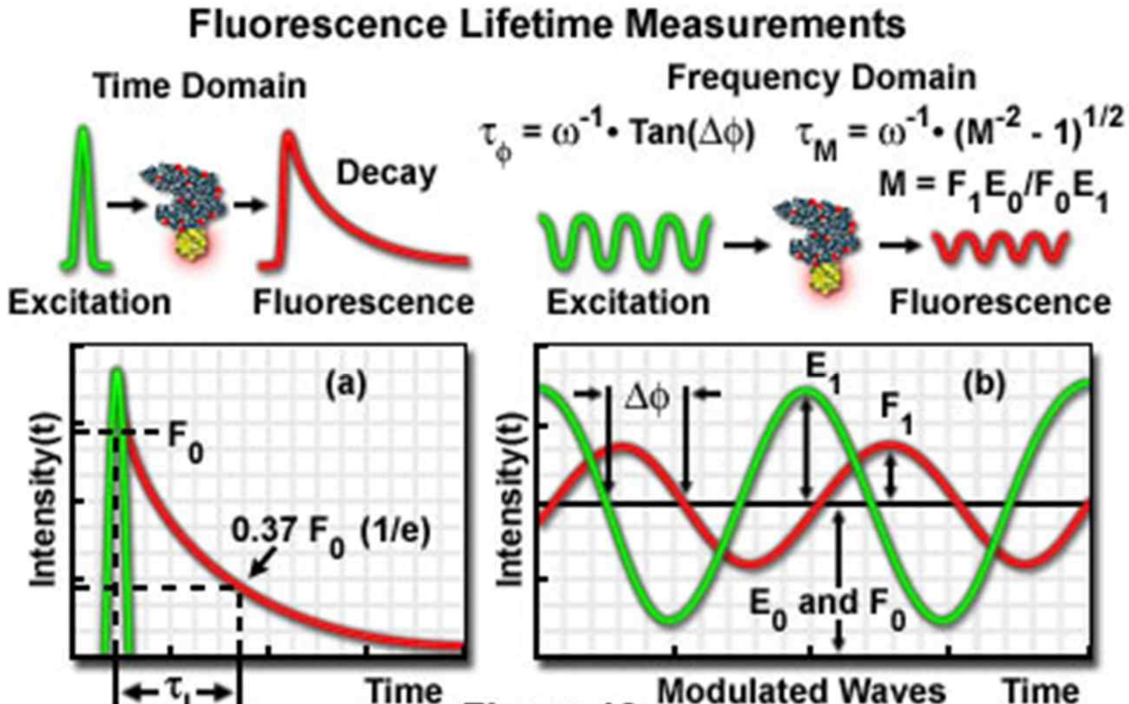

Fluorescence Lifetime Measurements
Time Domain
Decay
Excitation
Fluorescence
Frequency Domain
$\tau_\phi = \omega^{-1} \cdot Tan(\Delta\phi)$
$\tau_M = \omega^{-1} \cdot (M^{-2} - 1)^{1/2}$
$M = F_1E_0/F_0E_1$
Excitation
Fluorescence
(a)
Intensity(t)
F_0
$0.37\ F_0$ (1/e)
τ_l
Time
(b)
Intensity(t)
$\Delta\phi$
E_1
F_1
E_0 and F_0
Modulated Waves
Time

Figure 10

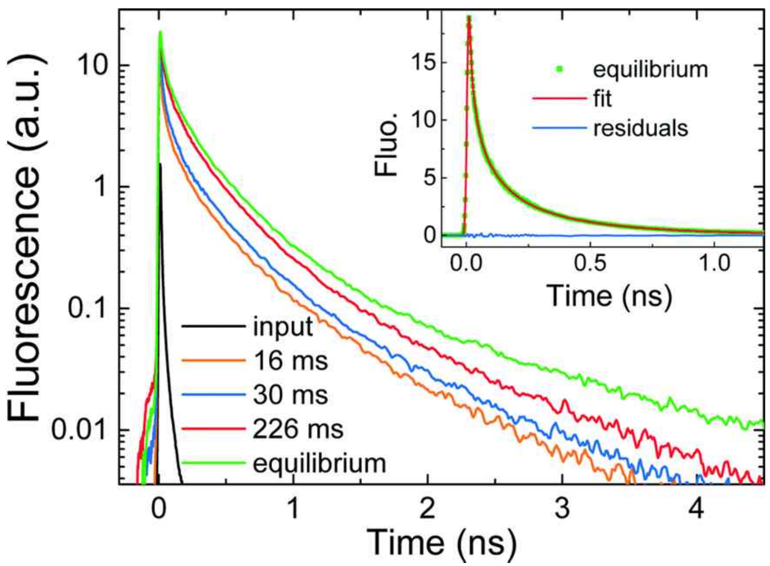

Fluorescence (a.u.)
10
1
0.1
0.01
input
16 ms
30 ms
226 ms
equilibrium
0
1
2
3
4
Time (ns)
Fluo.
15
10
5
0
equilibrium
fit
residuals
0.0
0.5
1.0
Time (ns)

Size and Shape Effects on Photoluminescence

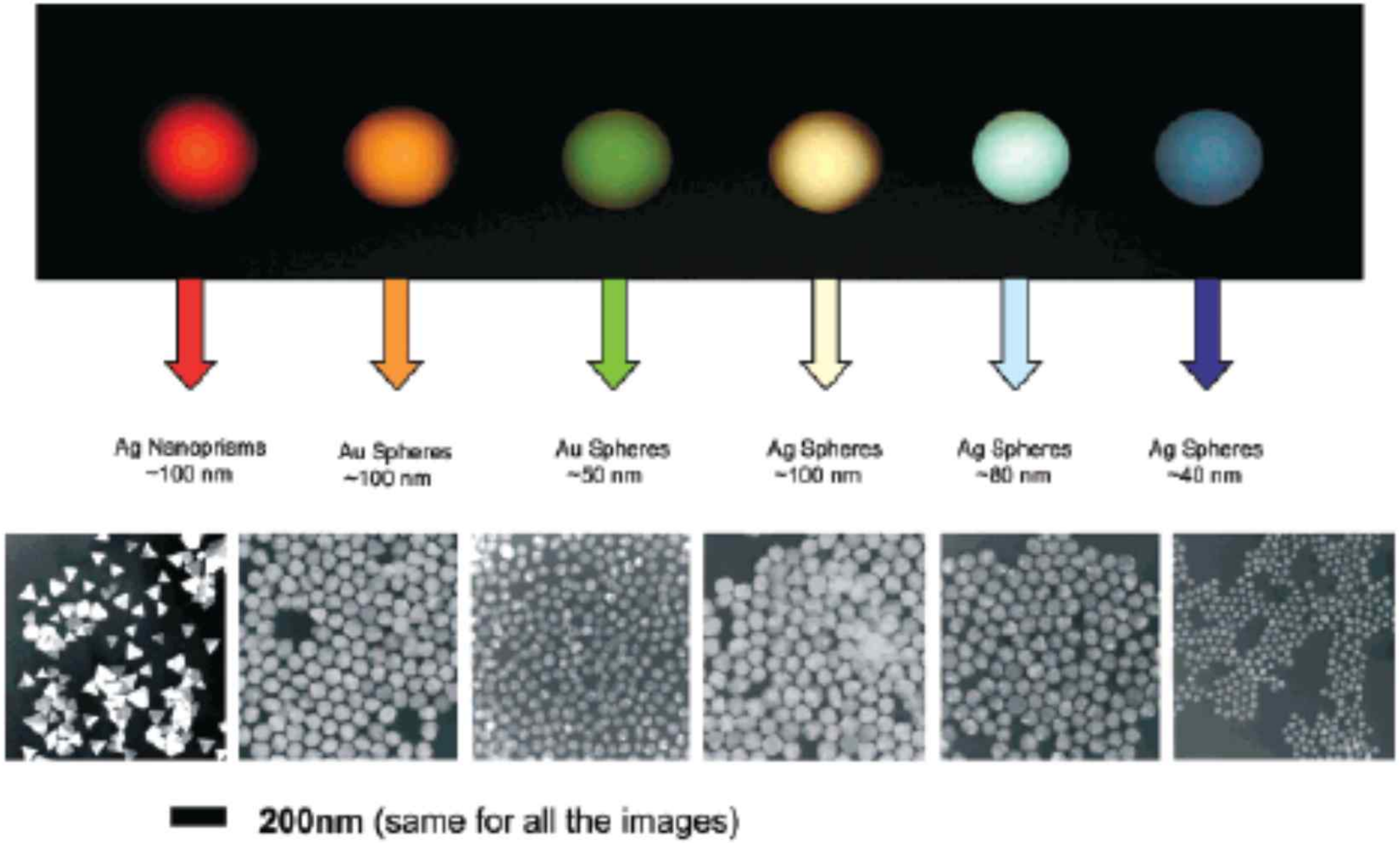

https://www.youtube.com/watch?v=6jSV6OV7rqE

Nanoelectronics, very strong and tough composites, functional nanostructured materials, etc

: from the effective separation of the spin and charge of an electron

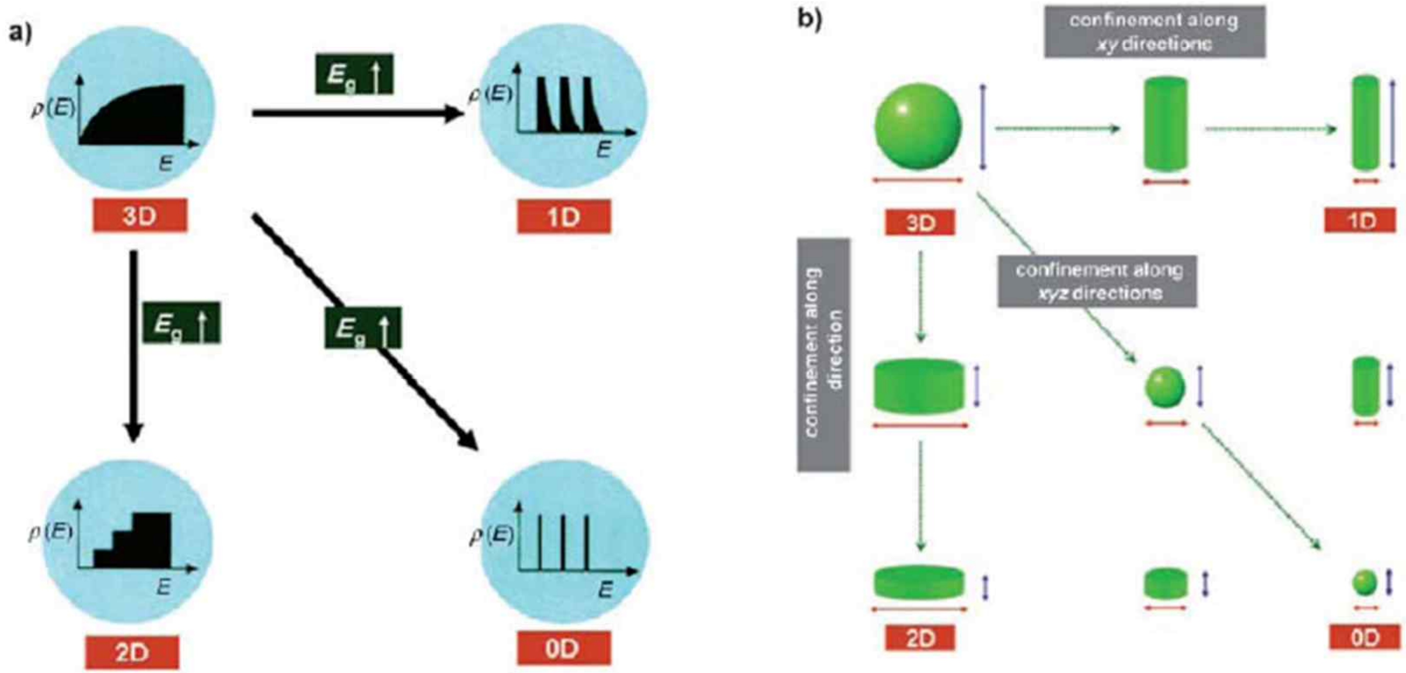

Figure 2. Shape evolution of crystals and their shape-dependent properties. a) The plot of density of state (DOS) versus energy is a continuous curve for 3D crystals and changes to a discrete line for 0D crystals. The band-gap energy of semiconductors and metal oxides gradually increases as the dimensionality and size reduce. b) Confinement of 3D crystals along one- (*z*), two- (*xy*), three (*xyz*) directions results in 2D, 1D, and 0D nanocrystals, respectively.

Professor Cheon (Yonsei University)
Angewandte Chemie, 45(21), 3414-3439 (2006)
J. Phys. Chem. B, 109 (31), 14795-14806 (2005)

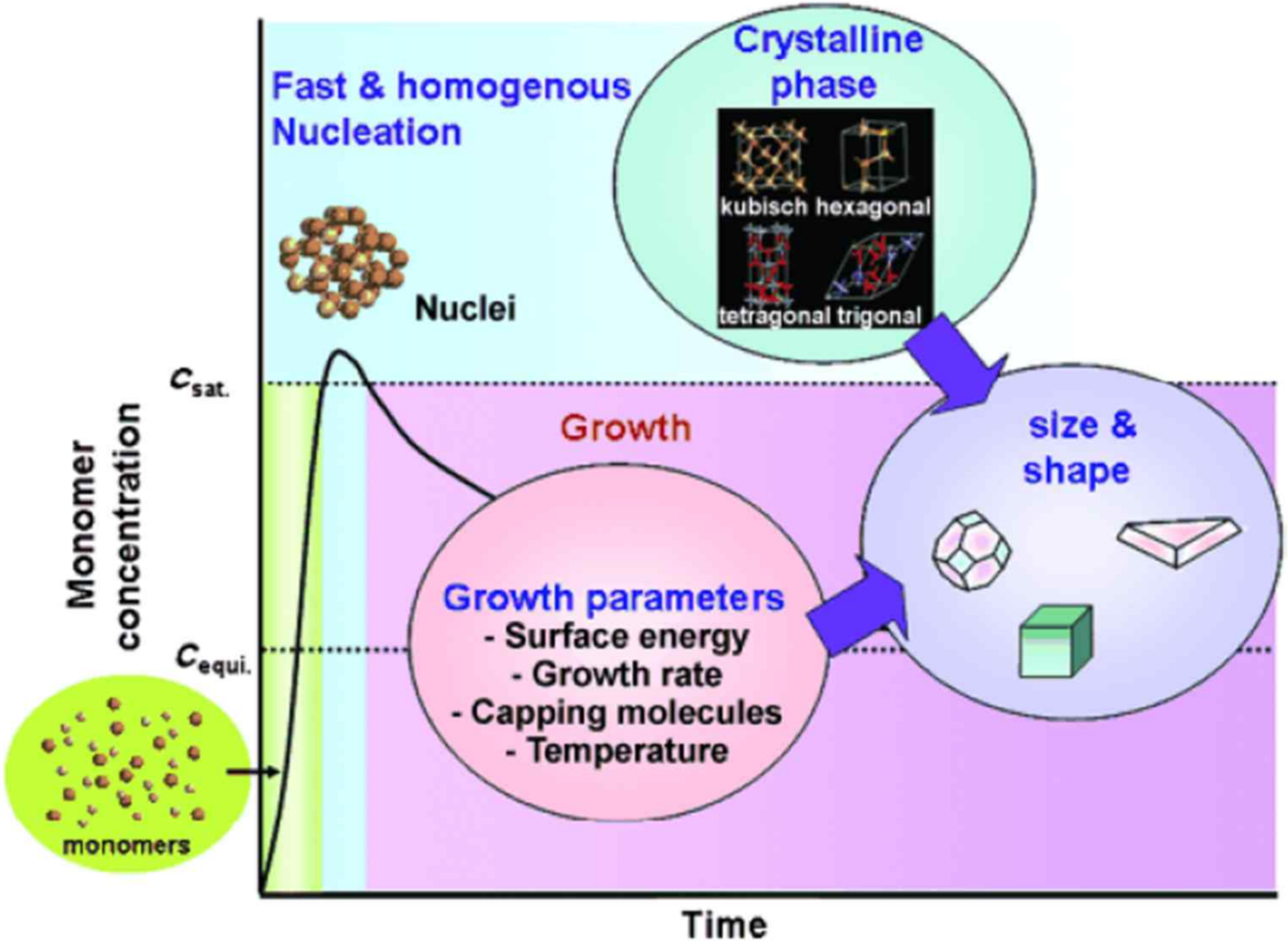

기존 균일한 나노입자의 제조과정과 그 문제점

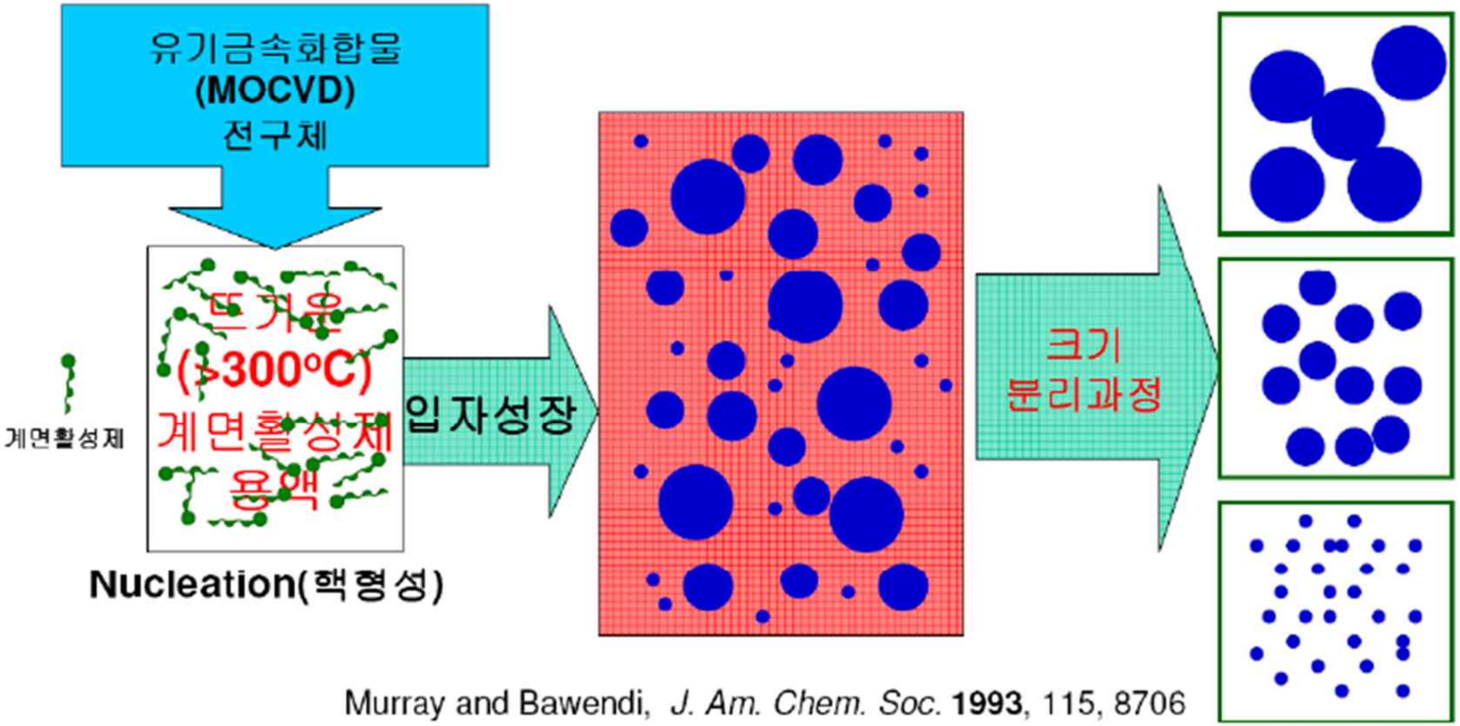

Murray and Bawendi, *J. Am. Chem. Soc.* **1993**, 115, 8706
Alivisatos, *J. Am. Chem. Soc.* **1998**, 120, 5343

균일한 나노결정입자가 아주 힘든 크기분리과정을 거쳐야만 가능하다 !!!

Key Issues in Nanoparticle Synthesis

- Size Uniformity
- Particle Size Control
- Shape control
- Large-scale Synthesis

Professor Hyeon (SNU)
Angewandte Chemie, 46,4630-4660 (2007)

Synthesis of Monodisperse Spherical Nanocrystals

*Jongnam Park, Jin Joo, Soon Gu Kwon, Youngjin Jang, and Taeghwan Hyeon**

Keywords:
gold · magnetic nanocrystals · monodisperse nanocrystals · noble metals · quantum dots · semiconductors

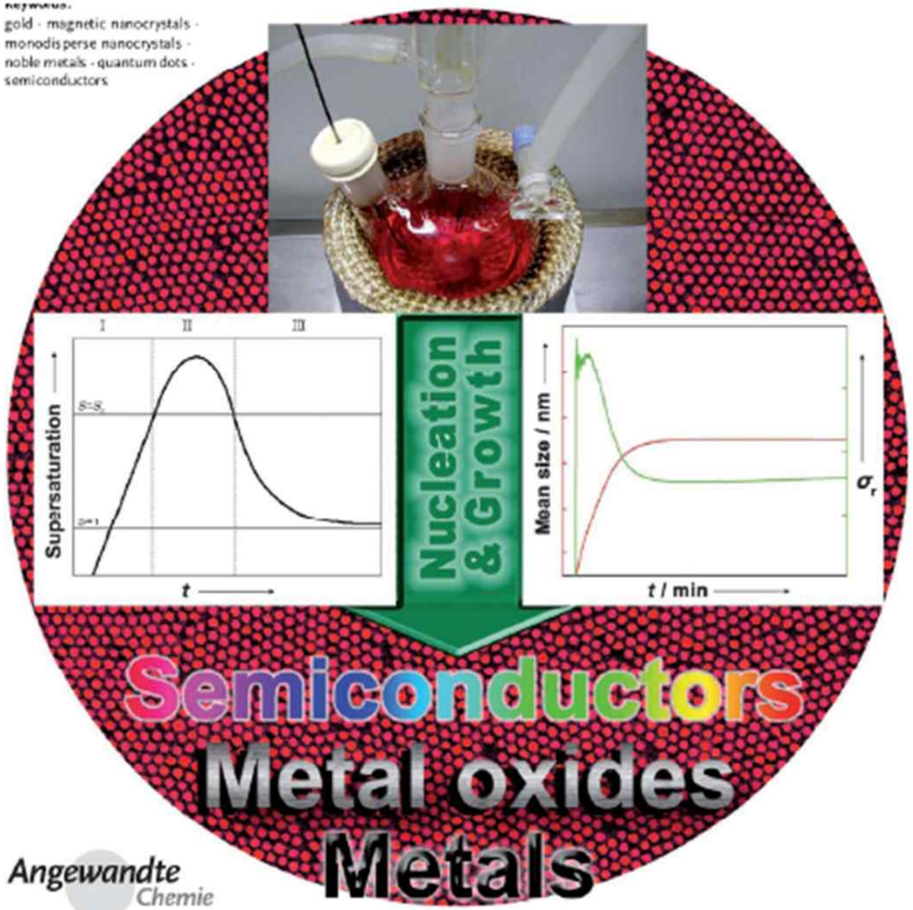

Angewandte Chemie

Direct synthesis of monodisperse, highly crystalline iron ferrite nanocrystals without a size-selection process

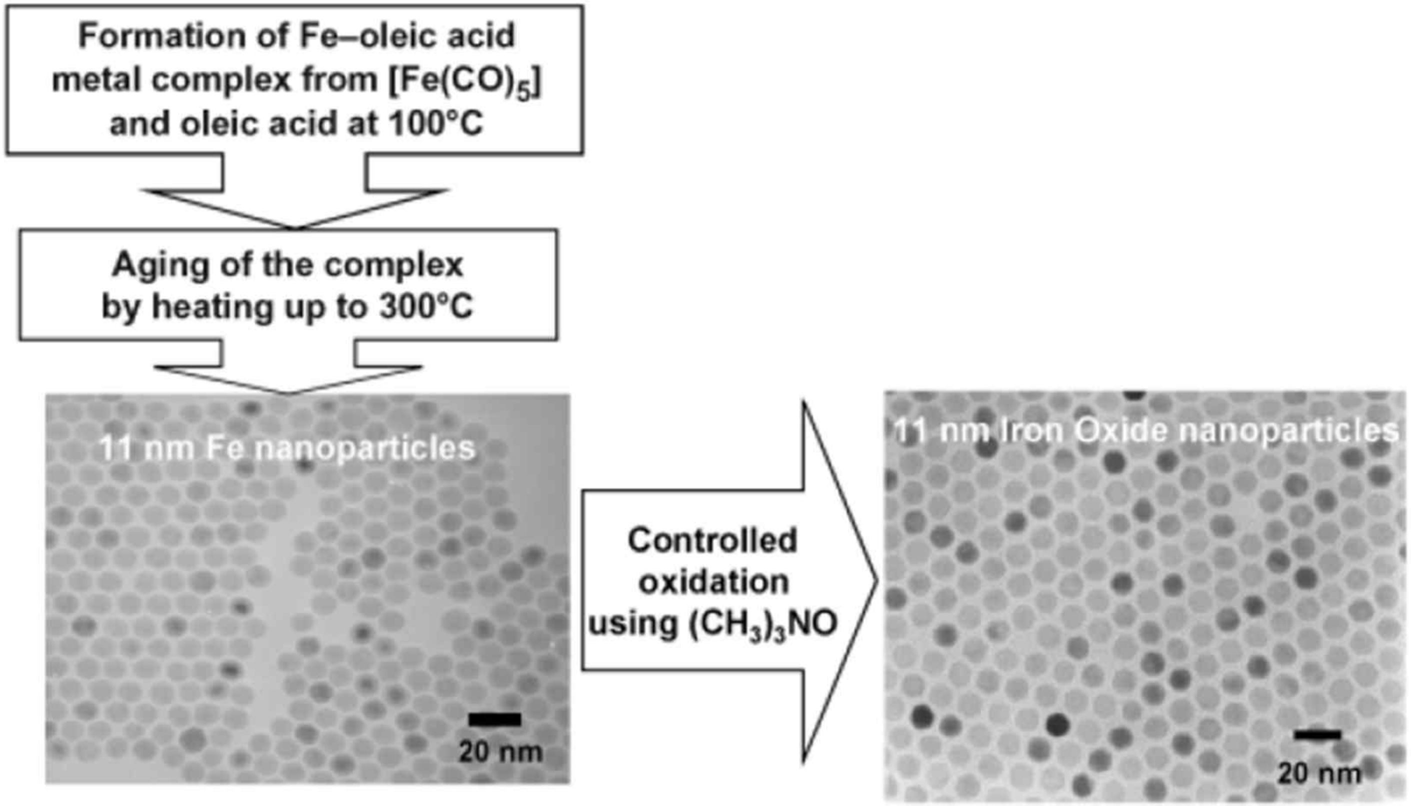

J. Park et al., Nature Materials, 2004, 3, 891

Size-controlled Synthesis of Monodisperse Iron Oxide Nanocrystals

Without a Size Selection Process!!!

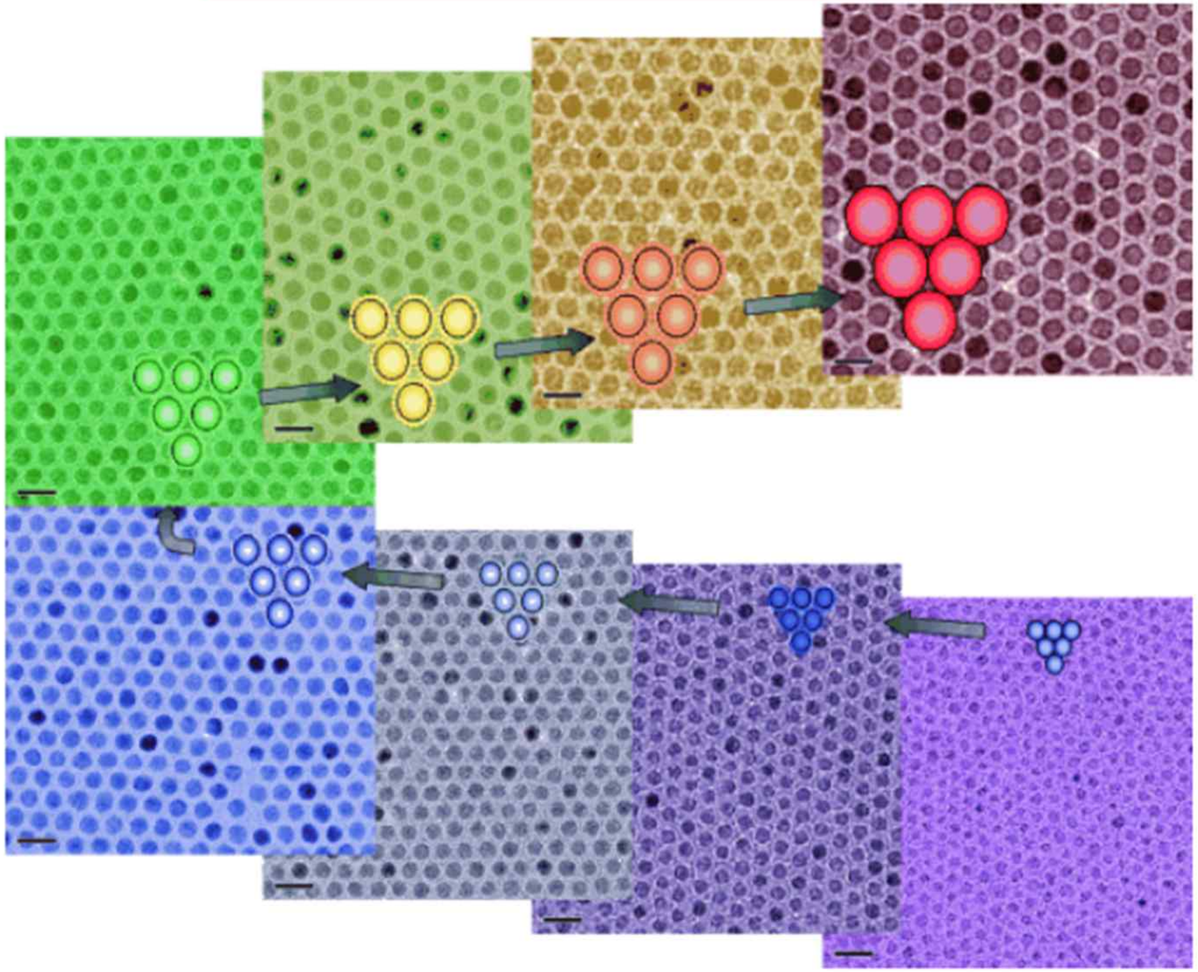

TEM images of iron oxide nanoparticles with particle diameters of 6, 7, 8, 9, 10, 11, 12, and 13 nm .

Ultra-large-Scale Synthesis of Uniform-sized Nanoparticles

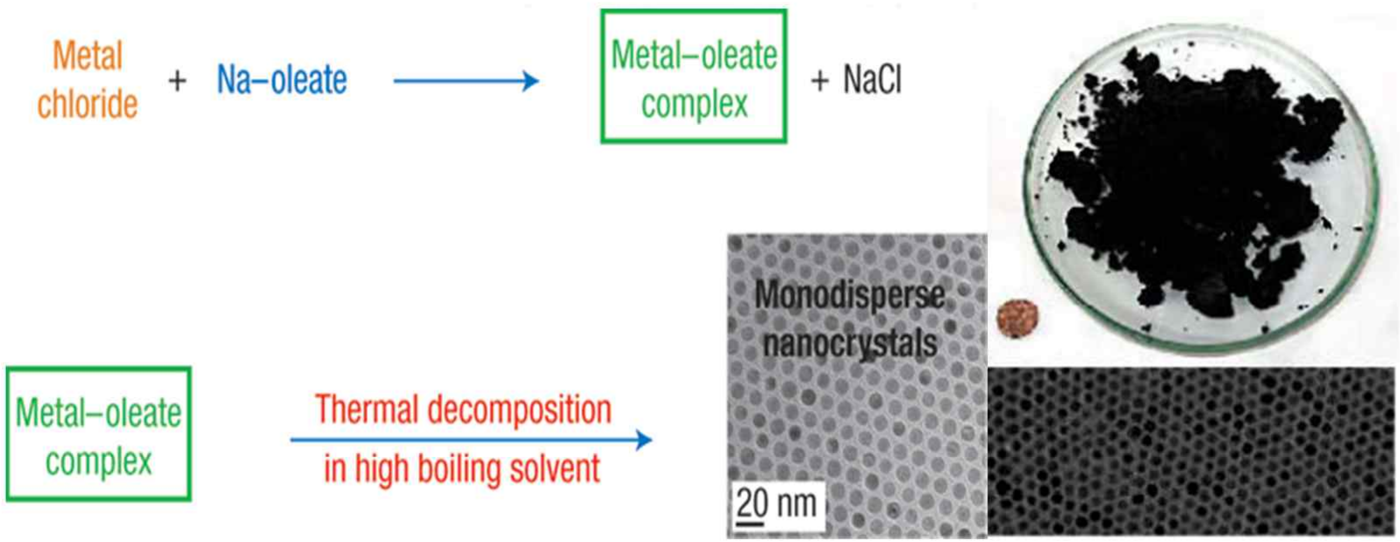

1) Large-scale Synthesis: 40 grams using 1 L reactor

2) Simple and Environmentally-Friendly process

3) Inexpensive using Hydrated Metal chlorides

J. Park *et al.*, *Nature Mater*. **2004**, 3, 891.

Table 1: Synthesis of monodisperse nanocrystals of metals and their oxides.[a]

Materials	Precursors/Reagents	Surfactants	Solvents	Method[b]	Ref.
Co	$CoCl_2/LiBEt_3H$	OLEA, TOP	OE	R	[27c]
	$Co(AOT)_2/NaBH_4$	NaAOT	H_2O, isooctane	R	[44]
Fe	$[Fe(CO)_5]$	OLEA	OE	T	[32a]
	$[Fe\{N(SiMe_3)_2\}_2]$	$C_{16}NH_2$, OLEA, HDAC	mesitylene	T	[47]
FePt	$[Fe(CO)_5]$, $[Pt(acac)_2]$/HDD	OLEA, OAm, HDD	OE	T, R	[2a]
	$[Fe(CO)_5]$, $[Pt(acac)_2]$	OLEA, OAm	dibenzyl ether	T	[49]
	$[Fe(acac)_2]$, $[Pt(acac)_2]$/HDD	OLEA, OAm, HDD	OE	R	[50]
CoPt, $CoPt_3$	$[Co_2(CO)_8]$, $[Pt(acac)_2]$/HDD	ACA, $C_{16}NH_2$, HDD	PE, *o*-dichlorobenzene	T, R	[51]
	$[Co(CO)_3NO]$, $[Pt(acac)_2]$/HDD	OLEA, OAm, HDD	OE	T, R	[52]
FeCoPt	$[Fe(CO)_5]$, $[Pt(acac)_2]$, $[Co(acac)_2]$/HDD	OLEA, OAm, HDD	OE	T, R	[53]
γ-Fe_2O_3	$[FeCup_3]$	TOA		T	[55]
	$[Fe(CO)_5]$/trimethylamine *N*-oxide	OLEA	OE	T	[32a]
	$[Fe(CO)_5]$/air	OLEA	OE	T	[57]
	$[Fe(acac)_3]$/HDD	OLEA, OAm, HDD	PE	R	[61]
	$FeCl_3 \cdot 6H_2O$, $FeCl_2 \cdot 4H_2O$	OLEA	ODE	T	[65]
	FeO(OH)	OLEA	ODE	T	[18c]
	$FeCl_3 \cdot 6H_2O$, $Na(OLEA)_3$	OLEA	ODE	T	[18a]
$CoFe_2O_4$	$[(\eta^5\text{-}C_5H_5)CoFe_2(CO)_9]$	OLEA	OE	T	[58]
	$[Co(acac)_2]$, $[Fe(acac)_3]$/HDD	OLEA, OAm, HDD	PE	R	[62]
$MnFe_2O_4$	$[Mn_2(CO)_{10}]$, $[Fe(CO)_5]$	OLEA	OE	T	[59]
	$[Mn(acac)_2]$, $[Fe(acac)_3]$/HDD	OLEA, OAm, HDD	PE	R	[62]
	$[Mn(acac)_2]$, $[Fe(acac)_3]$/HDD	OLEA, OAm, HDD	dibenzyl ether	R	[63]
TiO_2	$Ti(OiPr)_4$, $Ti(OnBu)_4$	Me_4NOH	H_2O, isopropanol	S	[68]
	$TiCl_4$, $Ti(OiPr)_4$	TOPO	heptadecane	N	[27a]
$BaTiO_3$	$BaTi(O_2CC_7H_{15})[OCH(CH_3)_2]_5/H_2O_2$	OLEA	PE	S	[69]
ZrO_2	$Zr(OiPr)_4$, $ZrCl_4$	TOPO		N	[27b]
HfO_2, $Hf_xZr_{1-x}O_2$	$Hf[OCH(CH_3)_2]_4(CH_3)_2CHOH$, $HfCl_4$	TOPO		N	[70]
Cu_2O	$CuSO_4$/sodium ascorbate	CTAB	H_2O	R	[73]
	$[Cu(acac)_2]$	OAm		T	[74]
	$Cu(OAc)_2$	TOA, OLEA		T	[75]
MnO	$Mn(OAc)_2$	TOA, OLEA		T	[76]
	$[Mn(acac)_2]$	OAm, H_2O		T	[77]
	$[Mn_2(CO)_{10}]$	OAm, TOP		T	[32b]
Mn_3O_4	$Mn(HCOO)_2$	OAm		T	[78]
FeO	$[Fe(CO)_5]$, $Fe(OAc)_2$, $[Fe(acac)_3]$	TOA, OLEA	OE	T	[79]
Co_3O_4	$[Co(NO_3)_2 \cdot 6H_2O$, $C_8H_{17}OH$		octanol	T	[80]
Ni	$[Ni(acac)_2]$	OAm, TOP		T	[81]
Sn	$[Sn(NMe_2)_2]_2$/HCl	$C_{16}NH_2$	toluene	T	[83]
	$Sn(NMe_2)_2$	PS-*co*-PVP	diisopropylbenzene, THF	T	[16b]
In	InCp	PVP, TOPO	anisole, toluene	T	[84]
	InCp	PVP	THF	T	[16b]
In_2O_3	$[In(acac)_3]$	OAm		T	[18b]
	$In(OAc)_3$/trimethylamine *N*-oxide	OAm, OLEA	hexadecane	T	[85]
Bi	$Bi[N(SiMe_3)_2]_3$	PS-*co*-PVP	diisopropylbenzene, THF	T	[16b]
Gd_2O_3	$Gd(Ac)_3 \cdot xH_2O$	OAm, OLEA	ODE	T	[86]
rare-earth oxide	Ln_2O_3,[c] $Ln(BA)_3(H_2O)_2$,	OAm, OLEA		T	[87]
CeO_2	$Ce(BA)_4$	OAm		T	[87]
CeO_2	$Ce(NO)_3$/PE	OAm, TOA		N	[88]

[a] For abbreviations, see the appendix at the end of this review. [b] T = thermal decomposition; R = reduction; N = nonhydrolytic sol–gel process; S = sol–gel process. [c] Ln = La, Pr, Nd, Sm, Eu, Gd, Tb, Er, Y.

Table 2: Synthesis of monodisperse semiconductor nanocrystals.

Materials	Precursors/Reagents	Surfactants	Solvents	Method[a]	Ref.
CdS	Me_2Cd, $(TMS)_2S$			T	[12a]
CdSe	Se, $(TMS)_2Se$	TOP, TOPO		T	[12a]
CdTe	Te, $(BDMS)_2Te$			T	[12a]
CdSe	Me_2Cd, Se	TBP, TOPO		T	[7]
InAs	$(TMS)_3As$, $InCl_3$	TOP		T	[7]
CdSe	Me_2Cd, Se	TOP, TOPO		T	[26b]
CdTe	$Cd(ClO_4)_2$, Al_2Te_3	thioglycolic acid		L	[26b]
InAs	$InCl_3$, $(TMS)_3As$	TOP		T	[26b]
CdSe	$Cd(Ac)_2$, $CdCO_3$, CdO, Se	TOPO, SA, LA, TDPA, $C_{12}NH_2$, TOP		T	[92b]
CdSe/ZnS	Me_2Cd, Se, Et_2Zn, $(TMS)_2S$	TOPO, TOP, $C_{16}NH_2$		T	[17a]
CdSe/CdS	$Cd(Ac)_2$, Se, H_2S	$C_{16}NH_2$, TOPO, TOP, TDPA		T	[93]
	CdO, Se, TBP, OLEA	SA, $C_{18}NH_2$, TOPO	ODE	T	[99]
CdS	CdO, S	OLEA	ODE	T	[92c]
	cadmium xanthate	$C_{16}NH_2$		T	[97]
CdTe	CdO, Te	TOPO, TOP, TDPA		T	[92a]
ZnSe	Et_2Zn, Se	TOP, $C_{16}NH_2$		T	[91]
ZnSe, ZnS	$Zn(SA)_2$, Se, S	$C_{18}NH_2$, TBP, SA	tetracosane, ODE	T	[96e]
PbS, ZnS, CdS, MnS	$PbCl_2$, $ZnCl_2$, $CdCl_2$, $MnCl_2$, S	OAm		L	[18d]
ZnS	Et_2Zn, S	$C_{16}NH_2$, OAm, OLEA	ODE	T	[103]
PbSe	$Pb(Ac)_2 \cdot 3H_2O$, Se	OLEA, TOP	PE	T	[96a]
	$Pb(Ac)_2 \cdot 3H_2O$, Se	OLEA, TOP	PE	T	[96c]
	PbO, Se	OLEA, TOP	ODE	T	[96d]
	$Pb(Ac)_2 \cdot 3H_2O$, Se	OLEA, TOP	PE	T	[105]
	$Pb(OLEA)_2$, Se	TOP	PE	T	[42a]
PbTe	$Pb(Ac)_2 \cdot 3H_2O$, Te	OLEA, TOP	PE	T	[96b]
Cu_2S	copper thiolate			T	[108, 109]

[a] T = thermal decomposition; L = Lewis acid–base reaction.

Table 3: Synthesis of monodisperse nanocrystals of gold, silver, and platinum group metals.

Materials	Precursors/Reagents	Surfactants	Solvents	Method[a]	Ref.
Au	$HAuCl_4$, $NaAuCl_4$/$LiAlH_4$	$C_{12}SH$, $C_{12}E_5$	hexadecane	R	[16d]
	$AuCl_3$/TBAB, hydrazine	$C_{12}SH$, $C_{12}NH_2$, DA	toluene	R	[17c]
	$HAuCl_4$	linoleic acid, sodium linoleate	EtOH, H_2O	T	[31f]
	$HAuCl_4$/$NaBH_4$, TOAB	$C_{12}SH$	toluene, H_2O	R	[123a]
	$HAuCl_4$/$NaBH_4$, acetic acid	*p*-mercaptophenol	MeOH	R	[123b]
	$HAuCl_4$/$NaBH_4$	poly(methacrylic acid)	H_2O	R	[123c]
	$[AuCl(PPh_3)]$/amine–borane	$C_{12}SH$, $C_{12}NH_2$, PPh_3	benzene, $CHCl_3$	R	[123d]
	$HAuCl_4$/$NaBH_4$, TOAB	$C_{12}SH$, $C_{18}SH$	toluene, H_2O	R	[125]
	Au	$C_{12}SH$	acetone, toluene	E	[126a]
	$AuCl_3$/$NaBH_4$	$C_{12}SH$, $C_{12}NH_2$, $C_{18}SiH_3$, TOP	toluene	R[b]	[126b]
	$AuCl_3$/$NaBH_4$	$(C_8–C_{16})SH$	toluene	R[b]	[126c]
	$HAuCl_4$/EG, Ag NPs	PVP	EG	R	[130, 132]
Pd	$[Pd(acac)_2]$/amine–borane	$C_{12}NH_2$	benzene	R	[123d]
	$PdCl_2$/alcohol	PVP	H_2O, MeOH, EtOH, 1-PrOH	R	[136]
	Na_2PdCl_4/EG	PVP	EG	R	[141]
	$[Pd(acac)_2]$	OAm, TOP	OAm, TOP	T	[144]
Ag	$Ag(Ac)_2$/TBAB, hydrazine	$C_{12}NH_2$, DA	toluene	R	[17c]
	$AgNO_3$	linoleic acid, sodium linoleate	EtOH, H_2O	T	[31f]
	$AgNO_3$/EG	PVP	EG	R	[40, 130]
	$AgCF_3COO$/amine–borane	$C_{12}SH$	benzene	R	[123d]
	$AgCF_3COO$	OLEA	isoamyl ether	T, R	[135]
Pt	$PtCl_4$/TBAB	$C_{12}NH_2$	toluene	R	[17c]
	Pt salt	linoleic acid, sodium linoleate	EtOH, H_2O	T	[31f]
	H_2PtCl_6/EG, metal salt	PVP	EG	R	[138, 139, 142]
Ni/Pd	$NiSO_4$, $Pd(Ac)_2$/polyol	PVP	dioxane, glycol	R	[137]
	$[Ni(acac)_2]$, $[Pd(acac)_2]$	TOP	OAm	T	[146]
Rh	$RhCl_3$/EG	PVP	EG	R	[143]
Ru	$RuCl_3$/polyol	Na(Ac), $C_{12}SH$	propanediol, EG, bis(2-hydroxyethyl) ether	R	[148a]
	$[Ru(cod)(cot)]$/H_2	PVP, $(C_8–C_{16})NH_2$, $(C_8–C_{16})SH$	THF	R	[147b]
PtRu	$[Pt(dba)_2]$, $[Ru(cod)(cot)]$/H_2	PVP	THF	R	[149]
Ir	$[(MeC_5H_4)Ir(cod)]$/HDD	OLEA, OAm	OE	R	[150]

[a] T = thermal decomposition; R = reduction E = solvated metal atom dispersion (SMAD) with subsequent digestive ripening; [b] reduction with subsequent digestive ripening.

Nanowires and Nanorods

Anisotropic nanocrystals including Nanorods and Nanowires are known to exhibit improved optical and magnetic characteristics compared to spherical counterparts.

Challenges

- Quantum sized nanorods and nanowires (usually diameters < ~ 20 nm)
- Diameter control
- Large scale synthesis

Strategies to Synthesize 1-D Nanostructures

Intrinsic anisotropic Crystallographic structure

Vapor-(or Solution) Liquid-Solid process

Using templates

Kinetic control by capping reagents

Oriented attachment

Size reduction from 1-D microstructure

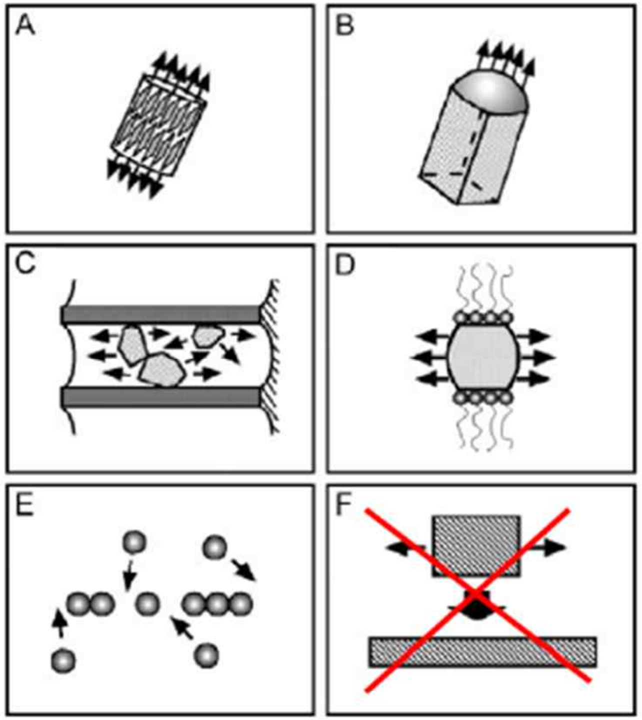

P. Yang and Y. Xia *Adv. Mater.* **2003**, 15, 353.

Shape Control of Semiconductor and Metal Oxide Nanocrystals through Nonhydrolytic Colloidal Routes

*Young-wook Jun, Jin-sil Choi, and Jinwoo Cheon**

Keywords:
colloids · metal oxides · nanostructures · semiconductors · shape control

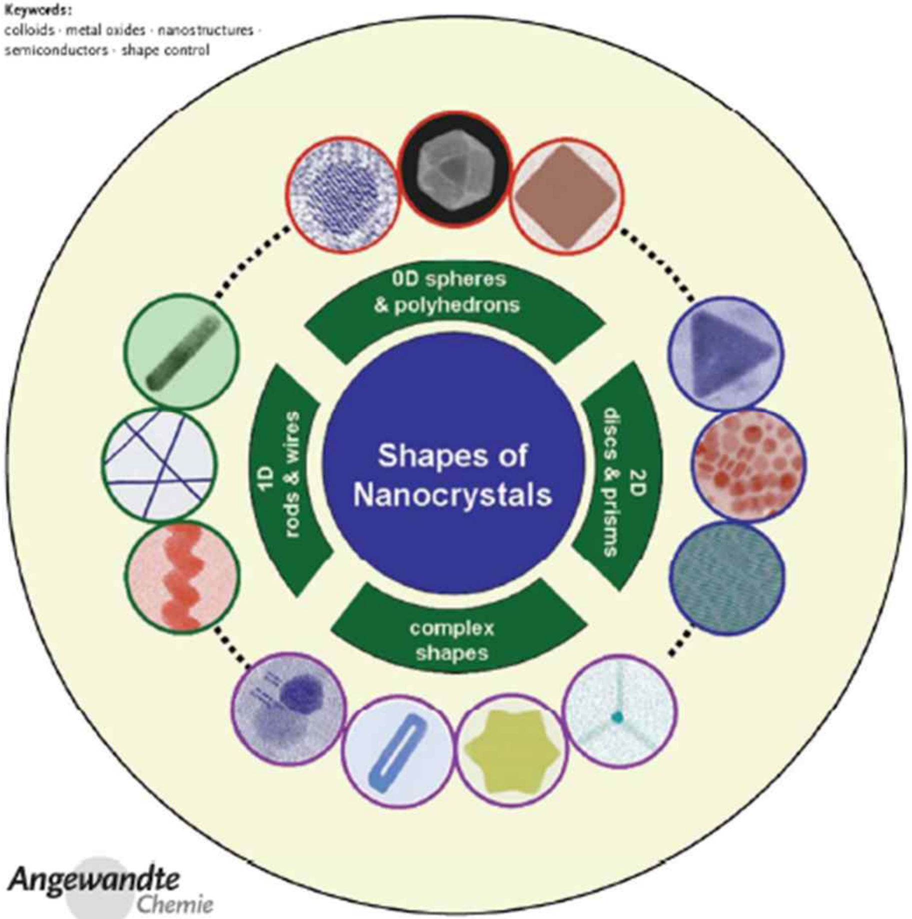

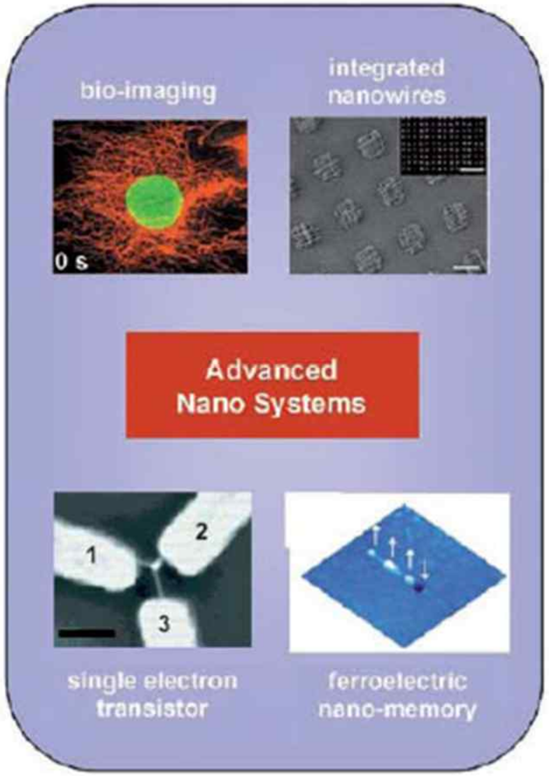

Angewandte Chemie

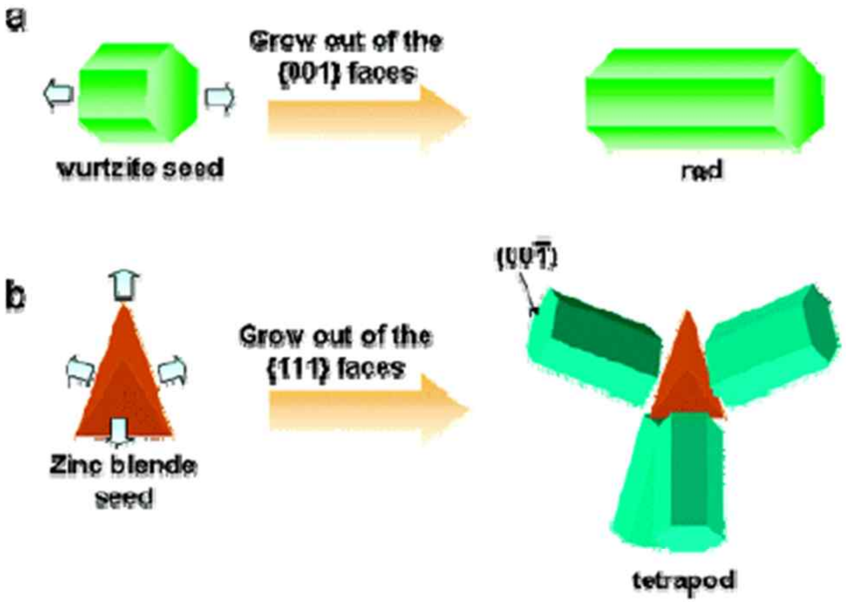

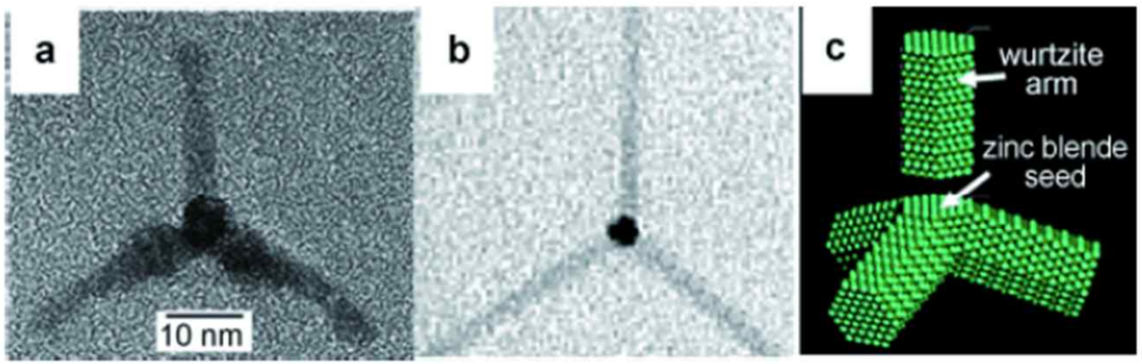

a) CdSe and b) MnS

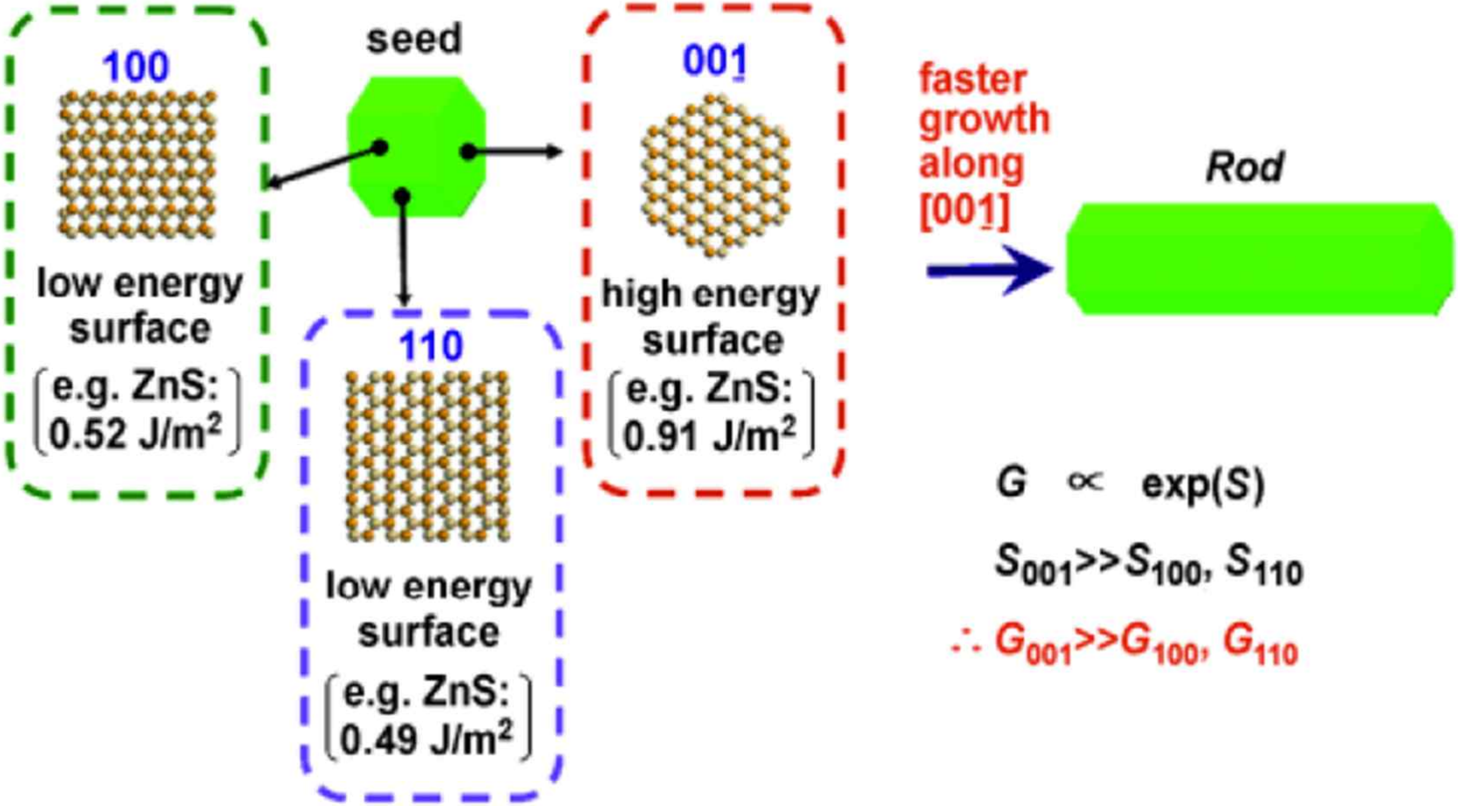

Surface energy of wurtzite ZnS nanocrystals. The (001) surface has the highest surface energy. Since the growth rate is exponentially proportional to the surface energy, the fastest growth occurs along the [001] direction in the kinetic growth regime; *G*=growth rate, *S*=surface energy.

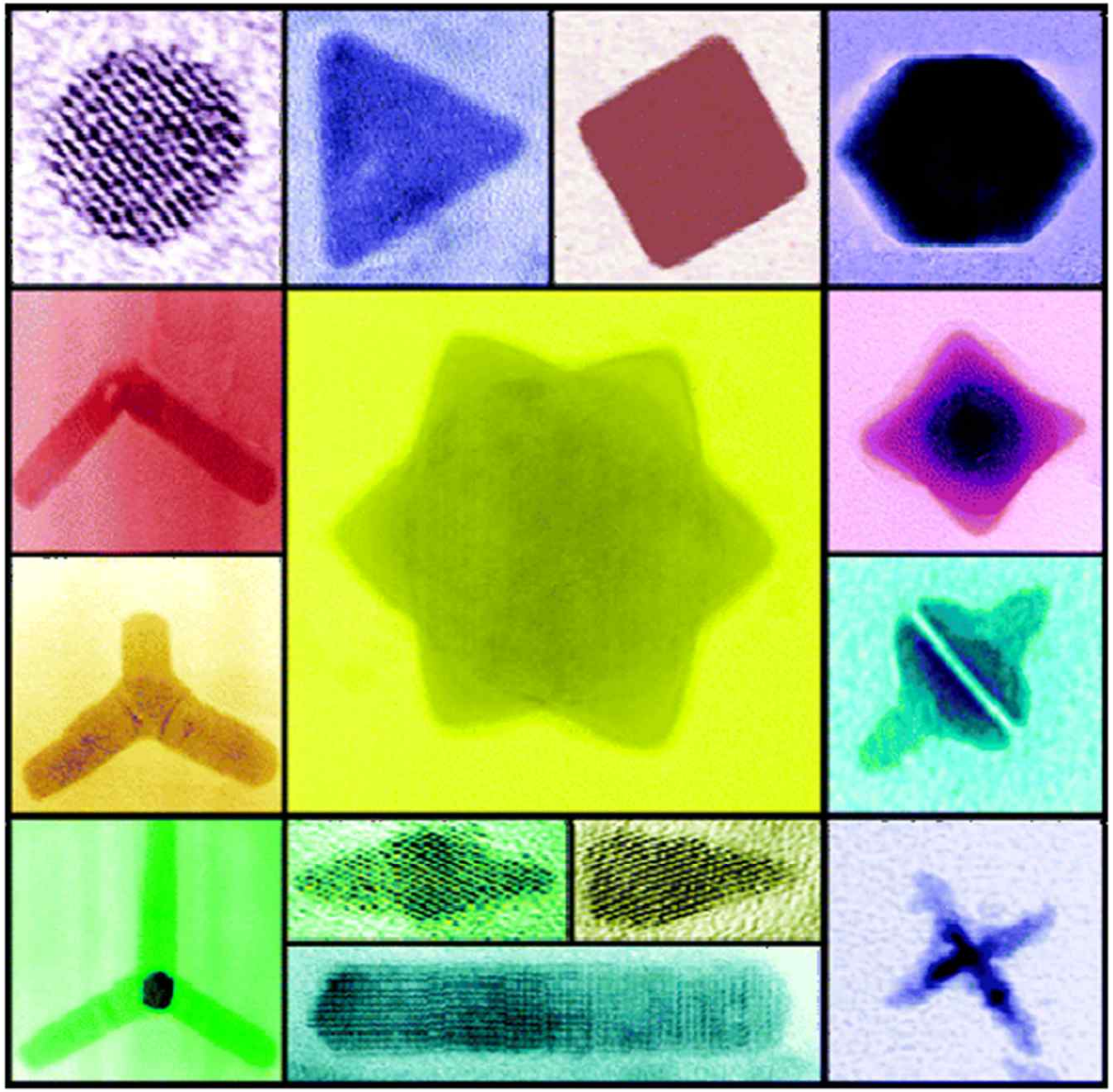

Fluorescent Nanoscale Materials

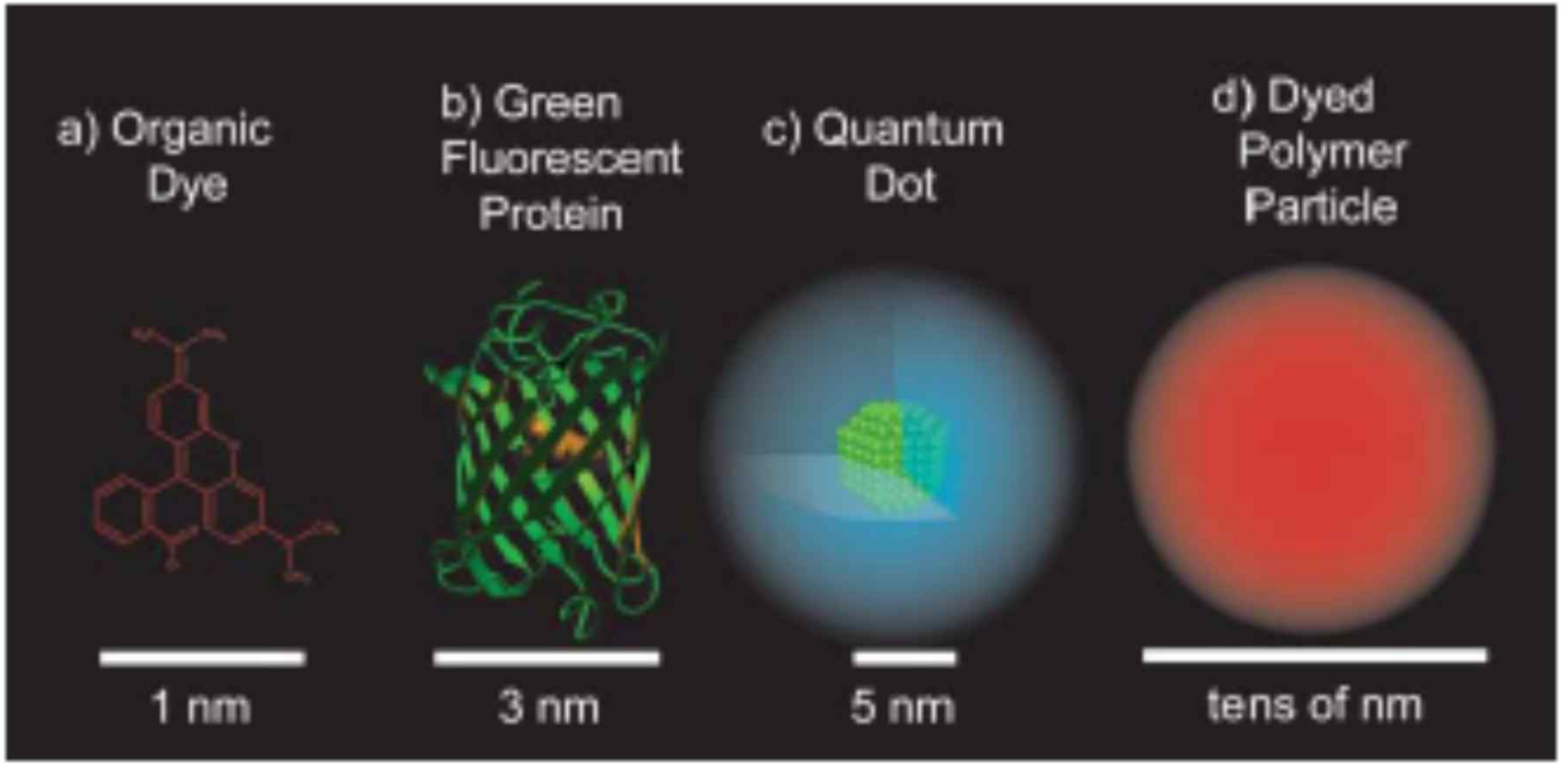

Mesoporous Silica Nanoparticles

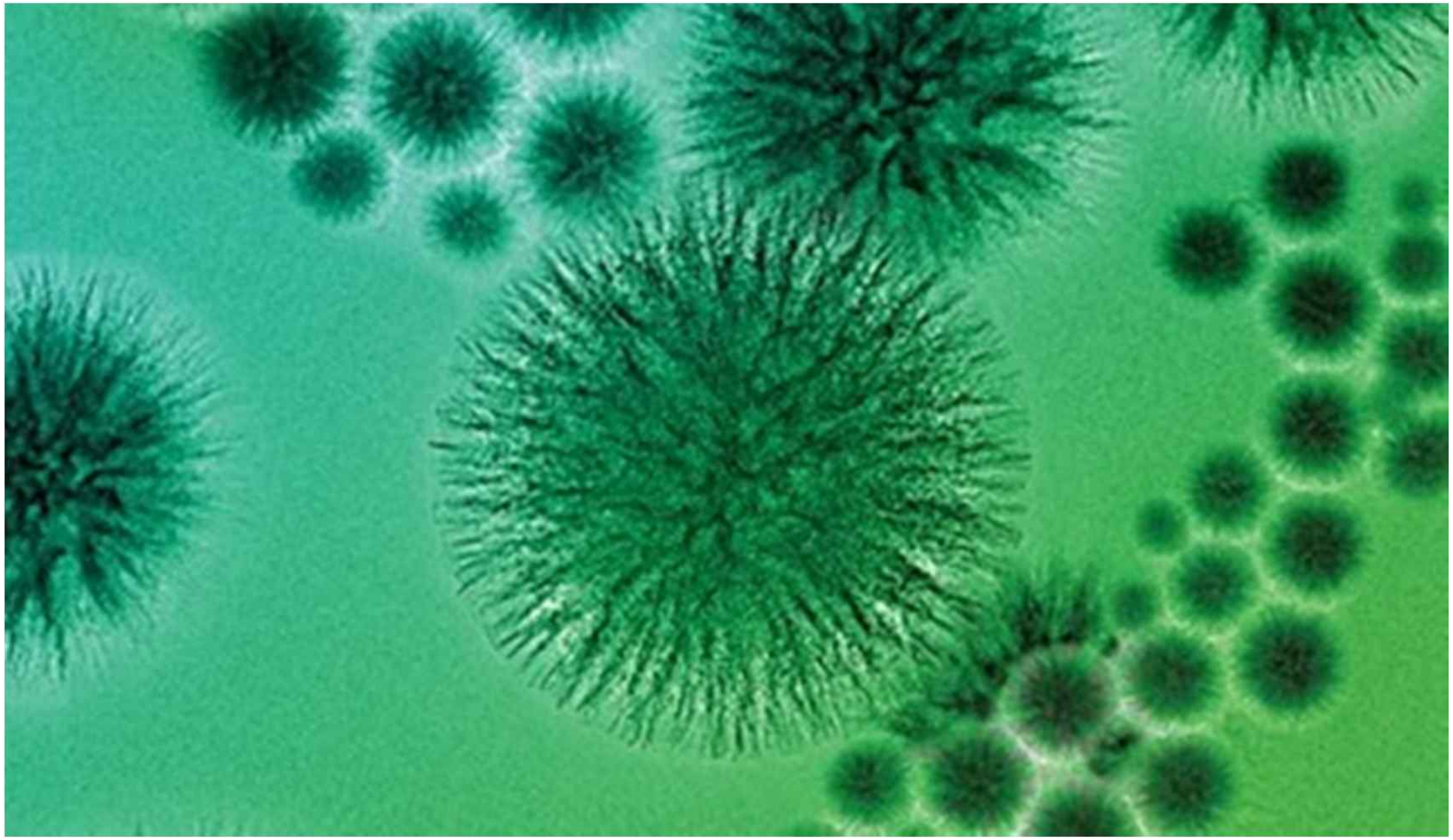

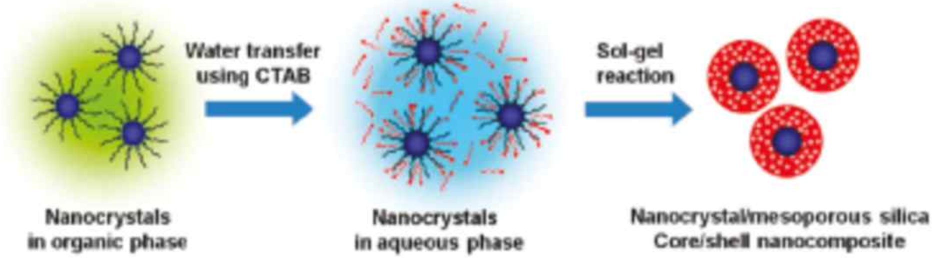

Functionalized Fluorescent Silica Nanoparticles

Ulrich Wiesner et al., Chem. Soc. Rev., 35, 1028 (2006)

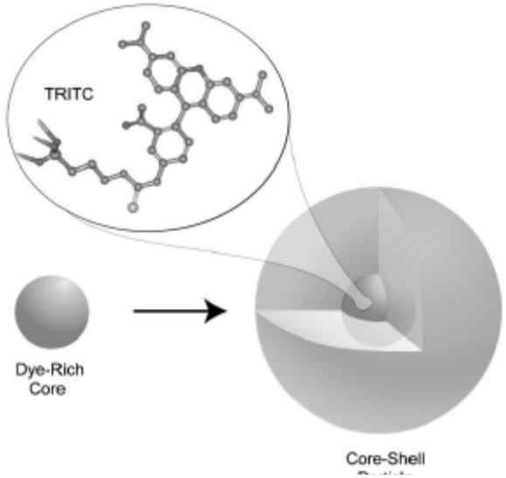

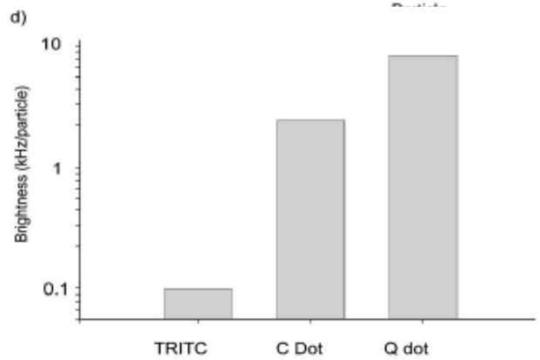

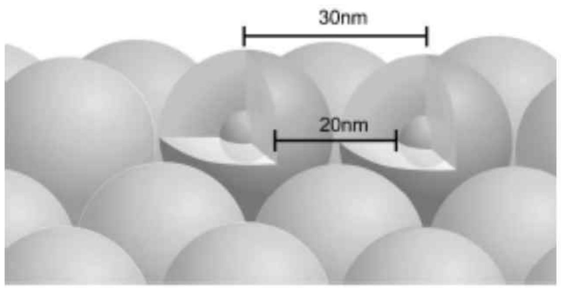

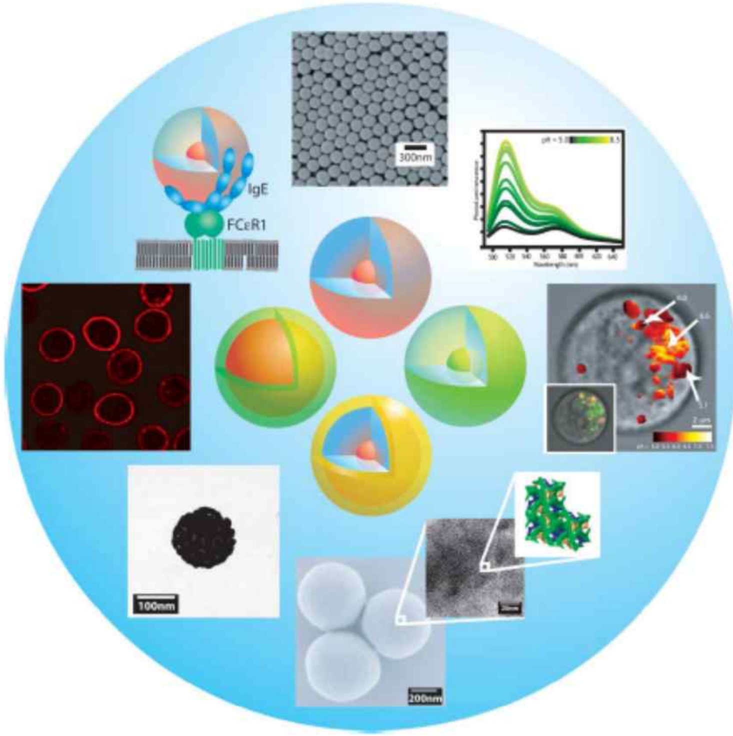

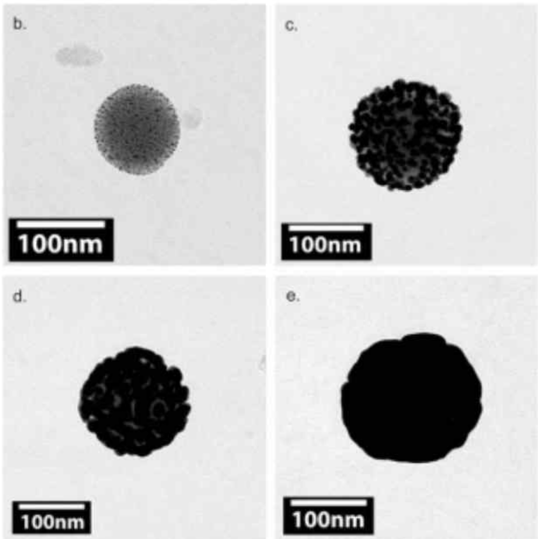

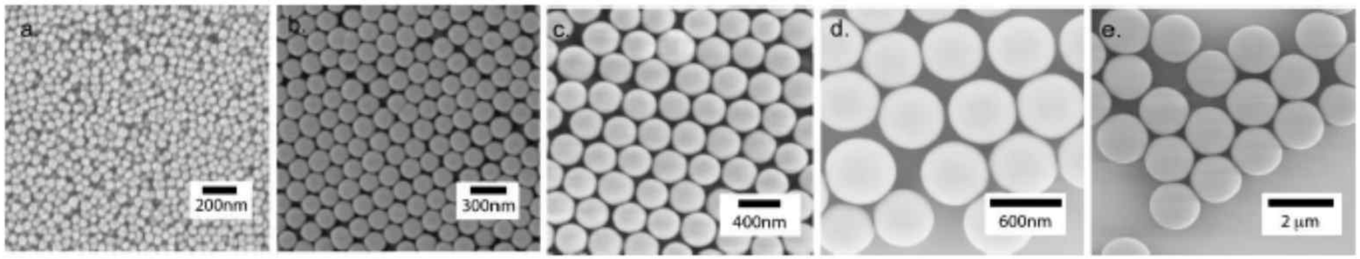

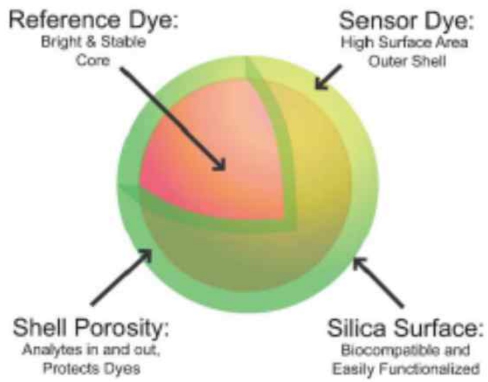
Reference Dye:
Bright & Stable Core
Sensor Dye:
High Surface Area Outer Shell
Shell Porosity:
Analytes in and out, Protects Dyes
Silica Surface:
Biocompatible and Easily Functionalized

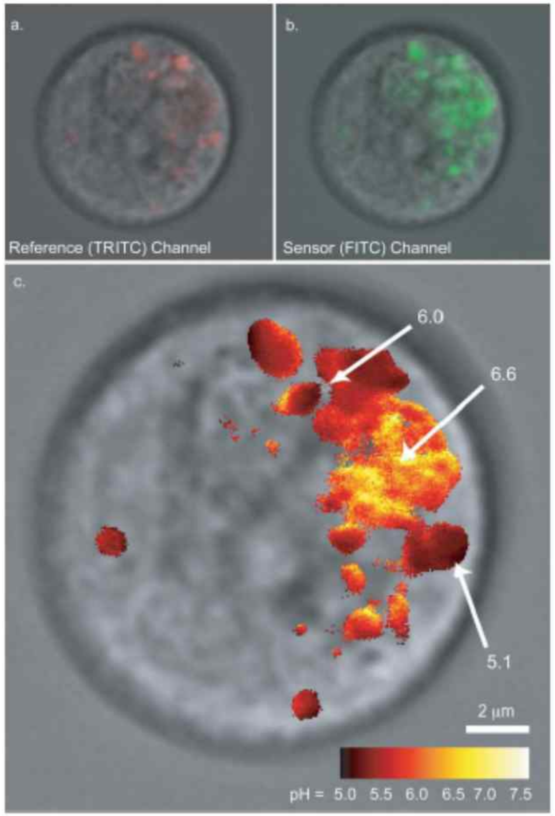
a.
Reference (TRITC) Channel
b.
Sensor (FITC) Channel
c.
6.0
6.6
5.1
2 μm
pH = 5.0 5.5 6.0 6.5 7.0 7.5

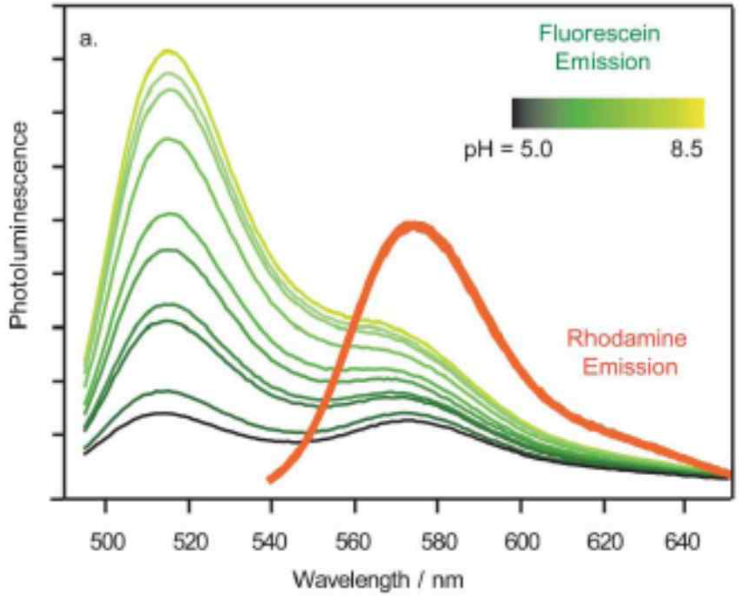
a.
Fluorescein Emission
pH = 5.0
8.5
Rhodamine Emission
Photoluminescence
500 520 540 560 580 600 620 640
Wavelength / nm

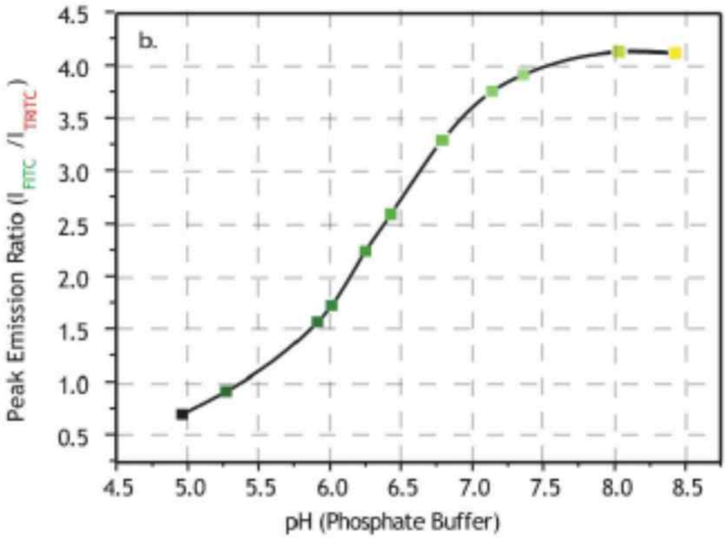
b.
Peak Emission Ratio (I FITC / I TRITC)
4.5 4.0 3.5 3.0 2.5 2.0 1.5 1.0 0.5
4.5 5.0 5.5 6.0 6.5 7.0 7.5 8.0 8.5
pH (Phosphate Buffer)

Theranosis Concept of Mesoporous Silica Nanoparticles

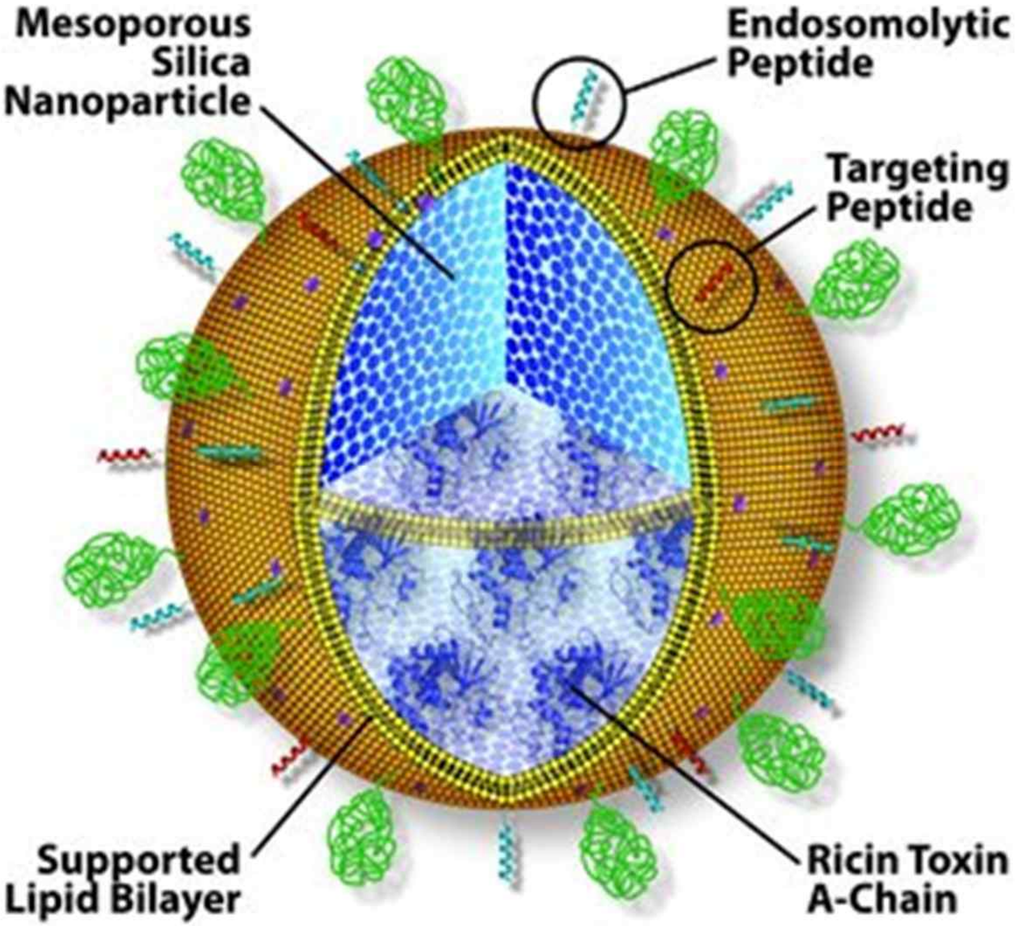

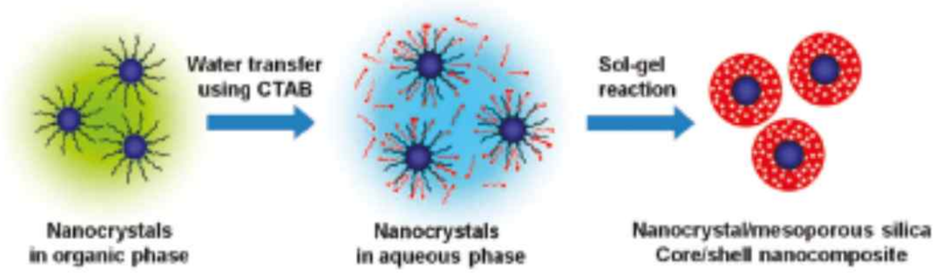

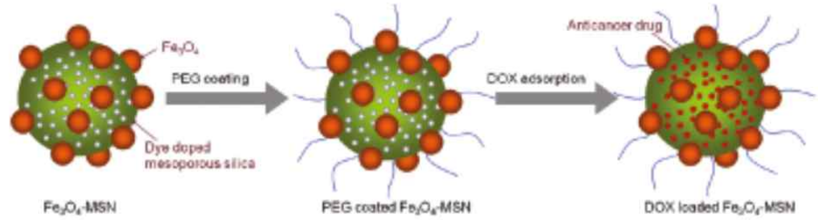

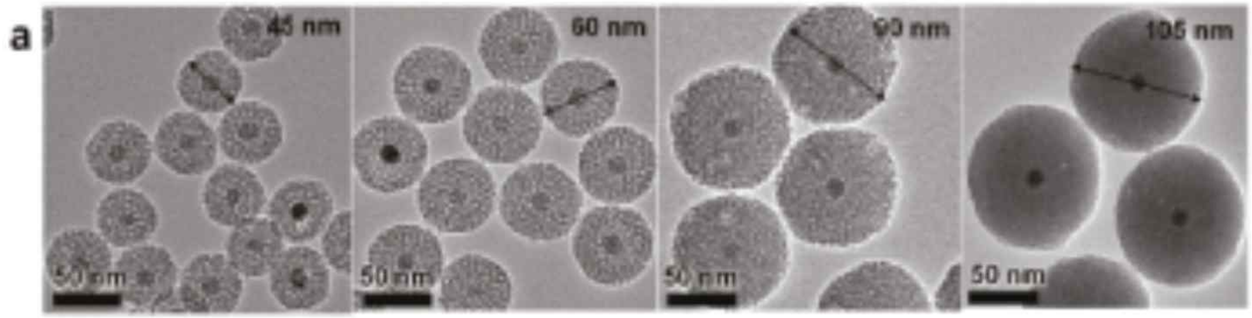

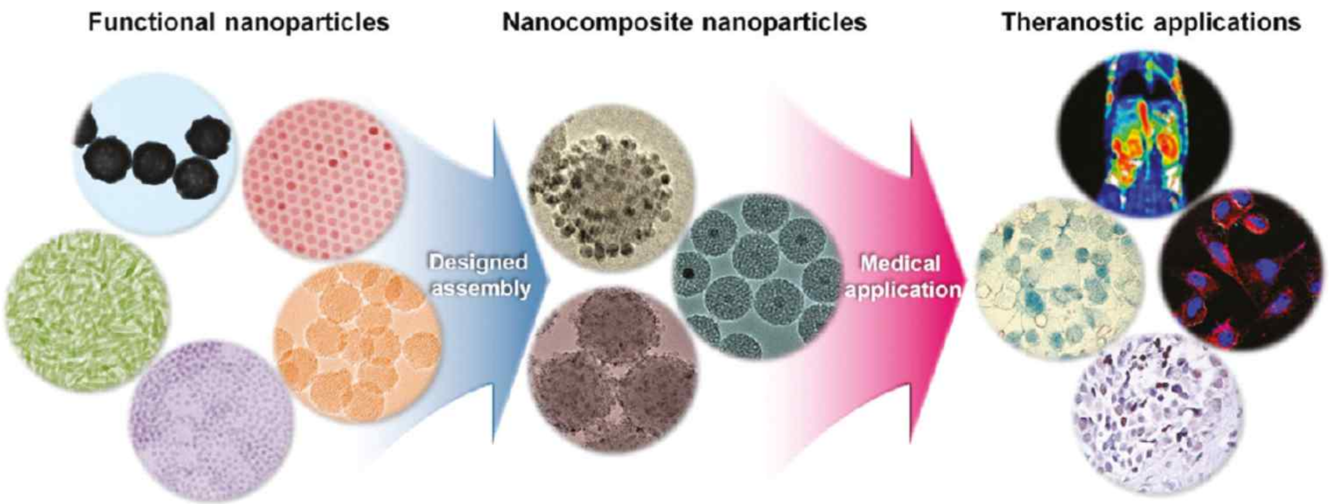

T. Hyeon et al., Acc. Chem. Res., 44, 893 (2011)